Copy No: _____

Dynamic Modelling of Cardiovascular Responses During Orthostatic Stress

Final Report

Ziren Lu, William Melek, Alex Kapps

Engineering Services Inc.
1 Bedford Rd, Unit 5
Toronto, Ontario Canada M5R 2J7

Contract Number: W7711-007683/A

Defence and Civil Institute of Environmental Medicine

Final Report
DCIEM-CR-2002-08
December 12, 2001

P517312.PDF [Page: 4 of 77]

104-05477/

Dynamic Modelling of Cardiovascular Responses During Orthostatic Stress

Final Report

Ziren Lu, William Melek, Alex Kapps

Engineering Services Inc
1 Bedford Rd, Unit 5
Toronto, Ontario Canada M5R 2J7

Project Manager: Dr. Alex Kapps, tel: (416) 595-5519, ext. 232

Contract Number: W7711-007683/A

Contract Scientific Authority: Dr. Bob Cheung, Head, Spatial Disorientation Group, Defence and Civil Institute of Environmental Medicine, 1133 Sheppard Avenue West, PO Box 2000, Toronto, ON M3M 3B9

The scientific or technical validity of this Contract Report is entirely the responsibility of the contractor and the contents do not necessarily have the approval or endorsement of Defence R&D Canada.

Defence and Civil Institute of Environmental Medicine (DCIEM)

Final Report
DCIEM-CR-
December 12, 2001

Author

Ziren Lu, William Melek, Alex Kapps

Engineering Services Inc

Approved by

Dr. Bob Cheung

Head, Spatial Disorientation Group, DCIEM

Approved for release by

F.J. (Fred) Maggio

Head, Aerospace Life Support Sector, DCIEM

Administrative Information

Project Manager	Dr Alex Kapps, tel: (416) 595-5519, ext 232 Engineering Services Inc 1 Bedford Rd, Unit 5 Toronto, Ontario Canada M5R 2J7
Contract Number:	W7711-007683/A
Contract Scientific Authority (CSA).	Dr Bob Cheung, Head, Spatial Disorientation Group, DCIEM

© Her Majesty the Queen as represented by the Minister of National Defence, 2001

© Sa majesté la reine, représentée par le ministre de la Défense nationale, 2001

P517312.PDF [Page: 6 of 77]

Abstract

This final report summarized the investigation of a subject's dynamic cardiovascular responses during orthostatic stress. For the purposes of this investigation, a toolbox dubbed CROST (*Countermeasures Research on Orthostatic Stress*) has been designed. The toolbox automatically generates and statistically analyzes dynamic models that reveal the dynamic behavior of the cardiovascular system during pitch and roll rotations: models for up/down tilt, pitch/roll rotations, different tilt onset/offset rates, and dwell times. The blood pressure dynamics is characterized by the physiologically significant indices associated with the models. Furthermore, using maneuver profile data, such as tilt orientation (pitch or roll), tilt direction (up or down), rotation rate (15, 30, 45 deg/sec) and head-down dwell time (7, 15, 30 sec) as well as the physiological indices, a set of fuzzy logic models is generated automatically by CROST. These dynamic and fuzzy-logic models assist in providing an operationally important predictive view on the characteristics of blood pressure responses to orthostatic stress induced by pitch and roll rotations.

Repeated measures analysis of variance has shown that the magnitude of blood pressure decrease induced by head-down tilt is significantly higher ($p < 0.05$) in pitch than in roll rotation, whereas the blood pressure decrease induced by the head-up (HU) rotation is significantly higher ($p < 0.05$) in roll than in pitch. The tilt orientation and rotation rate also have a significant effect on blood pressure dynamics. Our results demonstrate that the roll rotation to hypogravity followed by the pitch rotation back to hypergravity will induce the least decrease in a subject's blood pressure, thereby maximizing the subject's G-tolerance. The working hypothesis analyzed in this project is that the results can be explained on the basis of well-known otolith-cardiovascular reflex and bi-directional sensitivity of vestibular otolith organs that contribute to blood pressure compensation during pitch, but not during roll rotations.

Résumé

[Enter text: French]

This page is left blank

This page is left blank

P517312.PDF [Page: 9 of 77]

Executive summary

To generate and investigate dynamic models of cardiovascular responses during orthostatic stress, MATLAB-based computer package dubbed CROST (*Countermeasures Research on Orthostatic Stress*) has been designed and implemented. The toolbox possesses the following features and capabilities:

Graphic User Interface (GUI). User-friendly GUI automatically generates discrete/continuous time models from blood pressure time-series data. The models reveal the dynamic behavior of the cardiovascular system during pitch and roll rotations. A dedicated GUI performs various statistical analyses (e.g., paired T-tests and ANOVA repeated measures) on blood pressure signals and their associated indices.

Modeling the responses to pitch or roll motions. Models are generated to predict dynamic behavior of blood pressure responses to roll and pitch rotations for each subject: models for tilt-up/down, pitch/roll, different tilt onset/offset rates and dwell times. The behavior of blood pressure response is characterized by the indices associated with the models. These indices are automatically identified from the step response of the model. CROST also includes more advanced modeling techniques to automatically convert the developed model into a corresponding continuous-time transfer function and locate the model poles and zeros that are graphically displayed on the *s*-plane. Furthermore, the frequency response is derived and displayed using gain and phase margins Bode plots. Through such time series/frequency domain conversions, model parameters (step response characteristics, locations of poles and zeros, bode plots phase/gain margins) are identified for different tilt rates and dwell times.

Preprocessing and viewing input and output signals. CROST includes tools that acquire the user's knowledge (especially on physiological aspects) to improve the quality of the raw signal and/or fine-tune the model parameters. CROST also has various subroutines that work on raw input-output data to: (1) automatically adjust the sampling rate for blood pressure signals provided, (2) automatically select the suitable model prediction delay for every pressure signal based on the input-output data provided, (3) generate a discrete-time output error model based on the input-output data and output the corresponding parameters to the command window, (4) convert the discrete-time model in (3) to a continuous-time transfer function and outputs the locations of the corresponding poles and zeros, (5) model the difference between the pitch and roll responses.

Modeling the difference in responses to pitch and roll rotations. CROST can be used to generate separate dynamic models to identify the difference in blood pressure dynamics during pitch and roll rotations. This helps to investigate the directional selectivity of otoliths. The program allows the user to synchronize both pitch and roll signals at the start of tilt motion. The corresponding parameters for the model are automatically outputted to the MATLAB command window.

P517312.PDF [Page 10 of 77]

Furthermore, the step response of the identified discrete-time model is displayed for the analysis of otolith responses.

Statistical analysis. A statistical analysis toolbox was developed to analyze: (i) blood pressure signals recorded during tilt table or centrifuge experiments; and (ii) dynamic indices across subjects population. This subroutine was integrated with the MATLAB system identification GUI. CROST allows the user to perform statistical analysis of the dynamic indices obtained from models for all the subjects and reveal differences in the dynamic behavior of cardiovascular system during pitch and roll rotations.

Fuzzy-logic models. Using data on the tilt motion profile such as tilt orientation (pitch or roll) and tilt direction (up or down), rotation rate (15, 30, 45 deg/sec) and dwell time in head-down position (7, 15, 30 sec) as well as the physiological indices CROST derives from the dynamic models, a set of fuzzy logic models is generated automatically. The dynamic behavior of the cardiovascular system can be investigated by studying the rules that represent the fuzzy-logic models generated. The dynamic and fuzzy-logic models assist in providing an operationally important predictive view on the characteristics of blood pressure responses to orthostatic stress induced by pitch and roll rotations.

Repeated measures analysis of variance has shown that the magnitude of blood pressure decrease induced by head-down (HD) tilt is significantly higher ($p < 0.05$) in pitch than in roll rotation, while the decrease in blood pressure induced by the head-up (HU) rotation is significantly higher ($p < 0.05$) in roll than in pitch. The orientation and rotation rate also have a significant effect on blood pressure dynamics.

Generally, there exist four possible combinations of rotations during a G transition: (i) pitch during both transitions from +1 G_z to hypogravity and from hypogravity to +1 G_z; (ii) roll during both transitions from +1 G_z to hypogravity and from hypogravity to +1 G_z; (iii) pitch during transition from +1 G_z to hypogravity followed with roll during transition from hypogravity to +1 G_z; and (iv) (iii) roll during transition from +1 G_z to hypogravity followed with pitch during transition from hypogravity to +1 G_z. Our results show that among the four rotation combinations, roll rotation to HD and pitch rotation back to HU will induce the least decrease in blood pressure. Hence, G-tolerance is maximized by having a roll rotation during the hypergravity-to-hypogravity transition and a pitch rotation during the transition back to hypergravity. The maximum decrease in blood pressure occurs with pitch rotation to HD and roll rotation to HU. The working hypothesis analyzed in this project is that the results can be explained on the basis of well-known otolith-cardiovascular reflex and bi-directional sensitivity of vestibular otolith organs that contribute to blood pressure compensation during pitch, but not during roll. These results are being currently utilized in the design of operational recommendations for more G-tolerant operational flight regimes (e.g., split-S tactical maneuver) for combat aircraft than the ones currently in use.

P517312.PDF [Page: 11 of 77]

Table of contents

ABSTRACT i

EXECUTIVE SUMMARY iv

TABLE OF FIGURES vii

SOFTWARE USER MANUAL: *CROST TOOLBOX* 1

PAPER 1: *MODELING OF DYNAMIC CARDIOVASCULAR RESPONSES DURING G-TRANSITION INDUCED ORTHOSTATIC STRESS IN PITCH AND ROLL ROTATIONS* 25

PAPER 2: *DEPENDENCY OF CARDIOVASCULAR RESPONSES ON HEAD ORIENTATION IN HYPOGRAVITY AND HYPERGRAVITY TRANSITIONS* 56

P517312.PDF [Page: 12 of 77]

Table of figures

Figure 1: The setup for tilt-table experiments

Figure 2: Pitch and Roll rotations

Figure 3: A typical response of the BP in mm Hg recorded at heart level during pitch rotation (left) and roll rotation (right). Dotted line shows the profile of G transition during a complete tilt motion.

Figure 4: Model for subject 1 from HU-to-HD in pitch orientation (left). Model for subject 1 from HU-to-HD in roll orientation (right).

Figure 5: Model for subject 1 from HD-to-HU in pitch orientation (left). Model for subject 1 from HD-to-HU in roll orientation (right).

Figure 6: BP changes predicted by the models during HU-to-HD transition in pitch and roll rotations (left). BP changes predicted by the models during HD-to-HU transition in pitch and roll rotations (right)

Figure 7: An S-split maneuver and the corresponding G-force at every transition

Figure 8: The fuzzy input-output rules

Figure 9: Indices of a typical BP response to HU-HD and HD-HU transitions

Figure 10: comparison between the experimental data and the fuzzy models for pitch orientation

Figure 11: The fuzzy models of the pressure indices for pitch/roll rotations

Figure 12: the surface of the pressure indices obtained from fuzzy models for pitch/roll orientation

Figure 13: The effect of varying the dwell time on the pressure indices for pitch/roll orientation

ENGINEERING SERVICES INC. (ESI)
Automation & Robotics Systems

1 Bedford Road, Unit #5, Toronto, Ontario M5R 2J7, Canada
Telephone. (416) 595-5519 Facsimile. (416) 595-9994 URL http //www esit com

Dynamic Modeling Toolbox for investigation of *Cardiovascular Response Under Orthostatic Stress*

User's Manual

prepared for

Dr. B. Cheung, Head
Spatial Disorientation Group
Defense and Civil Institute of Environmental Medicine
1113 Sheppard Avenue West
Downsview, Ontario M3M 3B9

October 2001

P517312.PDF [Page: 14 of 77]

STEP 1.0

Click on the Matlab 5.3 icon located on the office toolbar at the right side of the screen. The **Matlab command** window will appear (leave this window open for the remainder of your session, because important messages may appear here).

STEP 2.0

- At the Matlab prompt (e.g.,>>) type <cd xxx > to the directory where the crost software is located.
- Type <crost1> and hit Enter. The **CROST Toolbox** window will appear

Fig. 1 Window 'CROST Toolbox'.

P517312.PDF [Page: 15 of 77]

STEP 3.0

If you want to model various CROST data using the system identification toolbox, left click on the button 'System Identification Analysis' (Fig. 1) and corresponding window will appear on the screen (Fig. 2). Otherwise, if you would like to perform statistical analysis on CROST data, left click on the button 'Statistical Analysis' and skip to step 9.0.

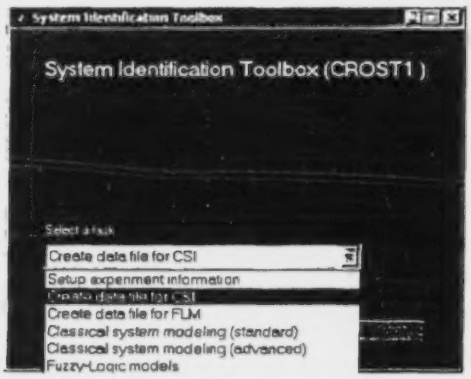
System Identification Toolbox (CROST1)
Create data file for CSI
Setup experiment information
Create data file for CSI
Create data file for FUM
Classical system modeling (standard)
Classical system modeling (advanced)
Fuzzy-Logic models

Fig. 2 Window 'System Identification Toolbox'.

STEP 4.0

If you are about to analyze a specific set of data, you can select option **Setup experiment information** *from* the drop-down menu. The experimental setup window will appear (*Fig. 3*); otherwise skip to step 5.0.

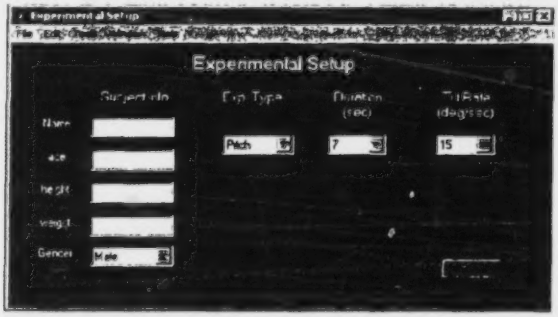

Fig. 3 Window 'Experimental Setup'.

Enter the relevant subject and experimental setup information and click on **Exit** when finished. You are ready to analyze data.

STEP 1.0

Click on the Matlab 5.3 icon located on the office toolbar at the right side of the screen. The **Matlab command** window will appear (leave this window open for the remainder of your session, because important messages may appear here).

STEP 2.0

- At the Matlab prompt (e.g.,>>) type <cd xxx > to the directory where the crost software is located.
- Type <crost1> and hit Enter. The **CROST Toolbox** window will appear

Fig. 1 Window 'CROST Toolbox'.

STEP 3.0

If you want to model various CROST data using the system identification toolbox, left click on the button 'System Identification Analysis' (Fig. 1) and corresponding window will appear on the screen (Fig. 2). Otherwise, if you would like to perform statistical analysis on CROST data, left click on the button 'Statistical Analysis' and skip to step 9.0.

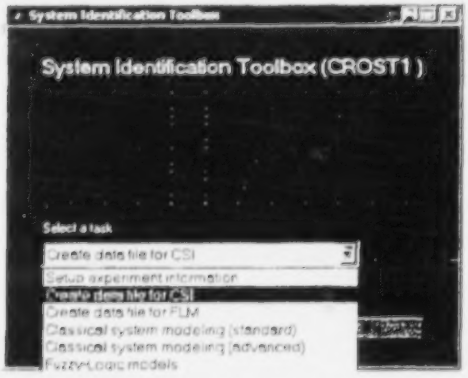

Fig. 2 Window 'System Identification Toolbox'.

STEP 4.0

If you are about to analyze a specific set of data, you can select option **Setup experiment information** from the drop-down menu. The experimental setup window will appear (Fig. 3); otherwise skip to step 5.0.

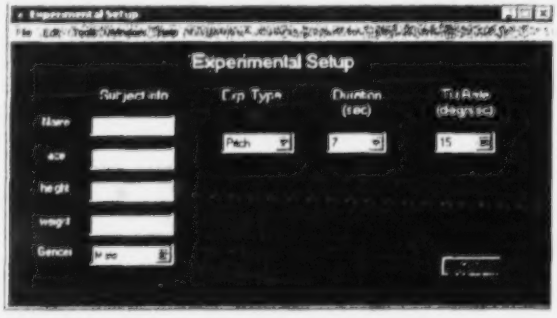

Fig. 3 Window 'Experimental Setup'.

Enter the relevant subject and experimental setup information and click on **Exit** when finished. You are ready to analyze data.

STEP 5.0

The system identification window (Fig. 2) in step 3.0 gives the user a tool to prepare data files for CSI (classical system identification) If for instance, it is chosen, the **Generate Data File** window (Fig. 4) will appear as shown below. The user can load raw data variables digitized for experimental charts (.out format for CROST experiments). To select a specific variable, i.e., systolic blood pressure, the user can locate such variable in the drop-down menu and select the corresponding channel number in the raw data. The explorer window will appear and user can then locate the raw variable and double-click to load it. If the process is completed successfully, the name of the variable will appear on the small window titled **Data inputted** on the **Generate Data File** window. Similar procedure can be followed to load other variables of interest (tilt profile, diastolic blood pressure, ECG, etc.).

For the purpose of classical system modeling analysis, it is recommended to generate a data file containing variables (ECG, systolic, diastolic, and tilt) for both orientation types, i.e., pitch and roll. In the example below, those variables were all selected for a specific subject (BC) at a dwell time of 7 seconds and a tilt rate of 45 deg. For convenience, the saved file is given the name bc1507.

After selecting all the variables to analyze from the explorer window, the User can click **save data** on the **Generate Data File** window. The software will automatically create .mat file that includes the selected subject's experimental variables. We are now ready to perform classical system identification analysis.

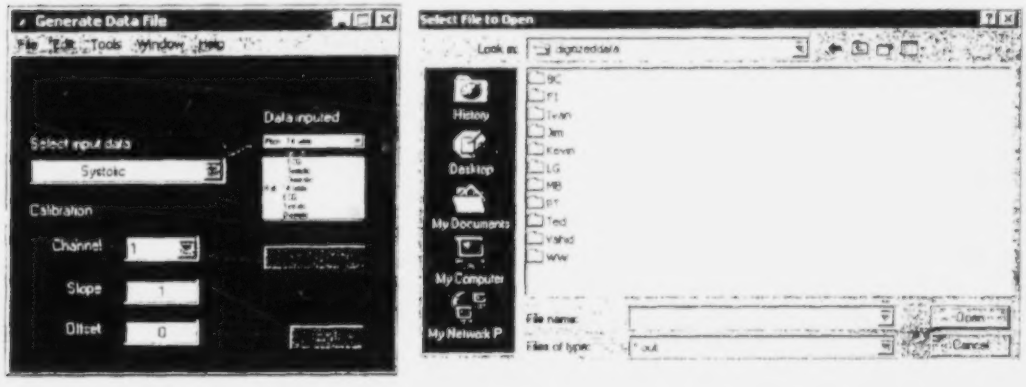

Fig. 4 Window 'Generate Data File'.

STEP 5.0

The system identification window (Fig. 2) in step 3.0 gives the user a tool to prepare data files for CSI (classical system identification) If for instance, it is chosen, the **Generate Data File** window (Fig. 4) will appear as shown below. The user can load raw data variables digitized for experimental charts (.out format for CROST experiments). To select a specific variable, i.e., systolic blood pressure, the user can locate such variable in the drop-down menu and select the corresponding channel number in the raw data. The explorer window will appear and user can then locate the raw variable and double-click to load it. If the process is completed successfully, the name of the variable will appear on the small window titled **Data inputted** on the **Generate Data File** window. Similar procedure can be followed to load other variables of interest (tilt profile, diastolic blood pressure, ECG, etc.).

For the purpose of classical system modeling analysis, it is recommended to generate a data file containing variables (ECG, systolic, diastolic, and tilt) for both orientation types, i.e., pitch and roll. In the example below, those variables were all selected for a specific subject (BC) at a dwell time of 7 seconds and a tilt rate of 45 deg. For convenience, the saved file is given the name bc1507.

After selecting all the variables to analyze from the explorer window, the User can click **save data** on the **Generate Data File** window. The software will automatically create .mat file that includes the selected subject's experimental variables. We are now ready to perform classical system identification analysis.

Fig. 4 Window 'Generate Data File'.

STEP 6.0

After generating a .mat data file(s) that includes experimental information for a subject. The user can select classical system modeling (standard) from the drop-down menu in step 3.0 to start analysis. Otherwise, if the advanced option is selected, skip step 6.0 and go directly to step 7.0.

If classical system modeling (standard) is selected, the **data fitting and modeling** window will appear as shown below. In this window, the user can load data files similar to those prepared in step 5.0 simply by clicking the **Load** button on the top right hand side of the window. Once the data file is selected, the name will be displayed for the user above the **Load** button.

After loading the file, the user has options to select the signal to be analyzed by various combinations. In the 'Direction' drop-down menu, the user can select: (i) HD (*head-down*) profile only, (ii) HU (*head-up*) profile only, or (iii) HU/HD (*head down and -up*)/complete profile. In the 'Orientation' drop-down menu, the user can select Pitch (*pitch-to-pitch*), Roll (*roll-to-roll*), Pitch/Roll (*pitch-to-roll*) or Roll/Pitch (*roll-to-pitch*) orientation. The following table summarizes the possible combinations.

Table 1: Matrix of Combinations of Direction and Orientation

	Down - Up	Down	Up
Pitch (pitch to pitch)	√	√	√
Roll (roll to roll)	√	√	√
Pitch/Roll (pitch to roll)	√		
Roll/Pitch (roll to pitch)	√		
Difference between Pitch and Roll		√	√

Once those selections are made, the can start modeling the corresponding signal.

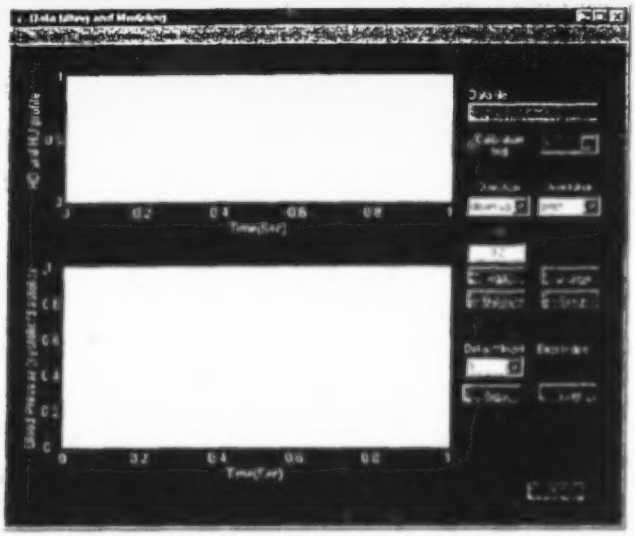

Fig. 5 Window 'Data Fitting and Modeling'.

In the example below, we loaded the subject file *bc1507*. We selected option down (HD) from the 'Direction' menu. We selected a roll signal for the orientation. The tilt scenario and the corresponding systolic pressure signal will be displayed for the user on the split plot window as shown below.

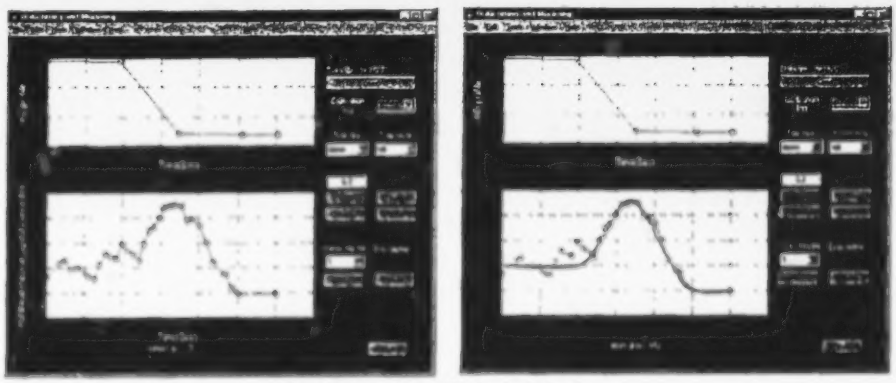

Fig. 6 Showing 'tilt-down' data.

To start modeling the selected pressure signal, the user must first select the sampling rate (default 0.2). Then, the user can start modeling by click on 'View'. However in many cases, the model performance is not satisfactory because of large noise in the signal. A tool to smooth out the noise is provided by locating key points in the signal such as initial value, peak point and final value, plus some points in transition period. Click the **Addt** button to select points of interest in the corresponding pressure signal. Once **Addt** button is clicked, a *cross* will appear on the window to allow the user to pick points of interest on the pressure signal, i.e., maximum drop in pressure, peak pressure, final status pressure, etc. To select a specific point, the user has to center the cross at the desired location and then left-click the mouse. The selected point will appear green on the figure. If a point is selected by mistake, the user can remove it by clicking the **delete** button option. If a point is accidentally misplaced on the figure, the user can relocate it using the **change** button option. Between two adjacent points selected by the user, the software will automatically perform spline interpolation to generate a nonlinear curve (in blue color).

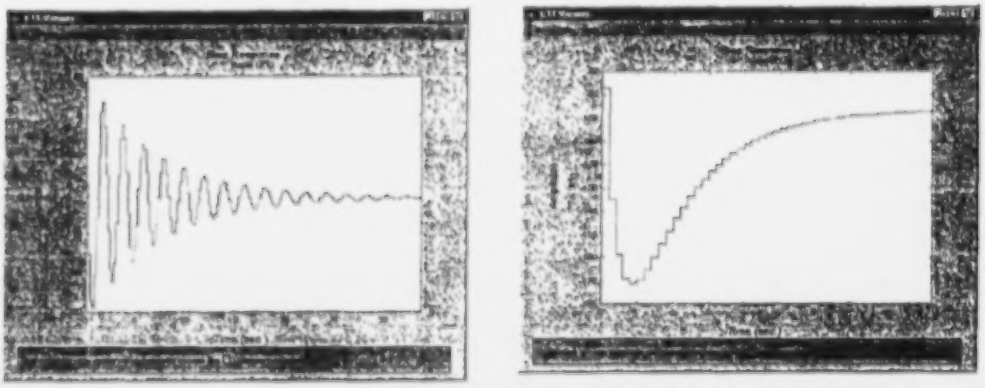

Fig. 7 Model outputs (left: using raw data; right: using filtered data).

Once those selections are made, the can start modeling the corresponding signal.

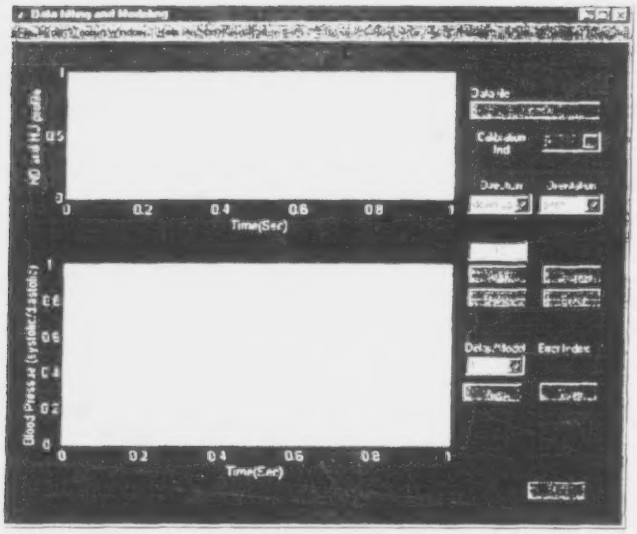

Fig. 5 Window 'Data Fitting and Modeling'.

In the example below, we loaded the subject file *bc1507*. We selected option down (HD) from the 'Direction' menu. We selected a roll signal for the orientation. The tilt scenario and the corresponding systolic pressure signal will be displayed for the user on the split plot window as shown below.

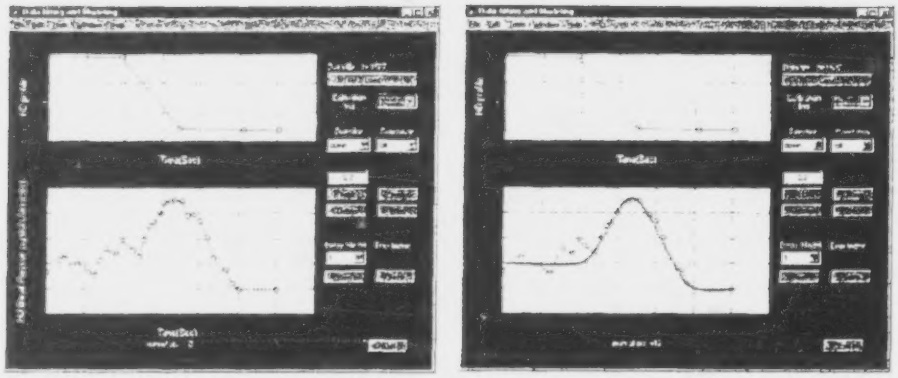

Fig. 6 Showing 'tilt-down' data.

To start modeling the selected pressure signal, the user must first select the sampling rate (default 0.2). Then, the user can start modeling by click on 'View'. However in many cases, the model performance is not satisfactory because of large noise in the signal. A tool to smooth out the noise is provided by locating key points in the signal such as initial value, peak point and final value, plus some points in transition period. Click the **Addt** button to select points of interest in the corresponding pressure signal. Once **Addt** button is clicked, a *cross* will appear on the window to allow the user to pick points of interest on the pressure signal, i.e., maximum drop in pressure, peak pressure, final status pressure, etc. To select a specific point, the user has to center the cross at the desired location and then left-click the mouse. The selected point will appear green on the figure. If a point is selected by mistake, the user can remove it by clicking the **delete** button option. If a point is accidentally misplaced on the figure, the user can relocate it using the **change** button option. Between two adjacent points selected by the user, the software will automatically perform spline interpolation to generate a nonlinear curve (in blue color).

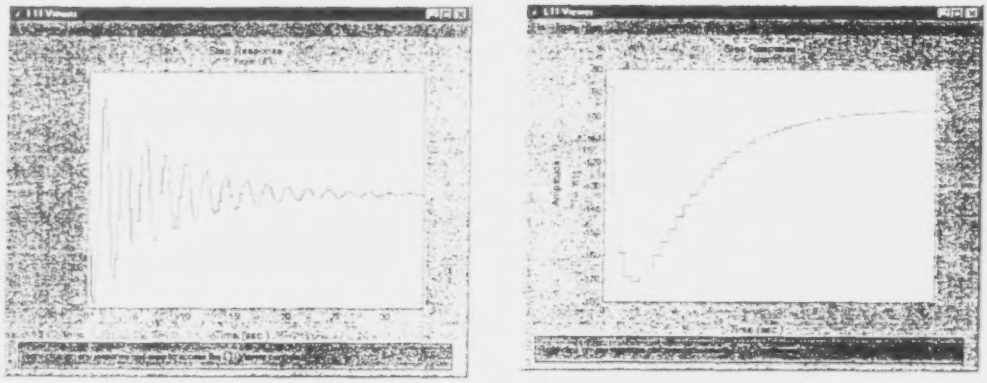

Fig. 7 Model outputs (left: using raw data; right: using filtered data).

P517312.PDF [Page: 20 of 77]

When all indices (points) of interest are selected from the signal, the user can select the **Enter** option. The complete spline curve generated by interpolation between selected points will be displayed in blue as shown below.

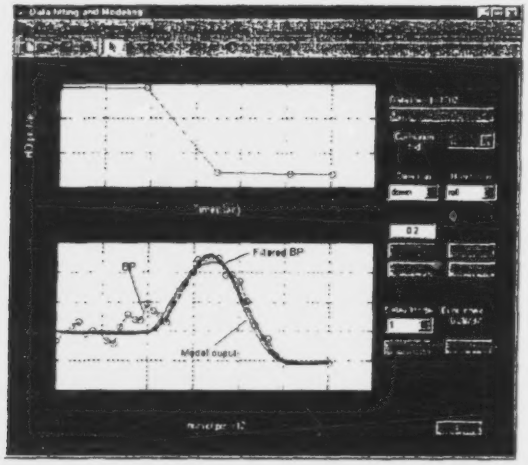

Fig. 8 Model output.

The blue curve generated above represents the filtered blood pressure signal without noise and outliers. Only meaningful pressure indices are picked by user and a smooth curve is fitted into them. To view the discrete-time second order model that represents the filtered blood pressure signal, the user has to first select the model prediction delay (default =1). The user can then click view and the model fit will be displayed in (light blue) as shown in the figure below. The sum of squared errors of the model vs. the filtered signal will also be displayed next to the model delay edit button..

If the model fit is not satisfactory, the user can relocate (change) some selected points to correct the model fit. Otherwise, if the fit is satisfactory, the user can click save button to store the corresponding second-order model parameters. Such parameters are indices located by user on the actual signal, model damping coefficient, model natural frequency, output-input model gain, and discrete-time prediction delay.

STEP 7.0

If the **system modeling (advanced)** option is selected in the system identification drop-down menu in step 3.0, a **select analysis** window will appear as shown below. In part 1 (Get Data), the user can create a .mat data file in a procedure identical to that in step 5.0. Otherwise, the user can load an existing .mat file that was generated on a previous system identification analysis run.

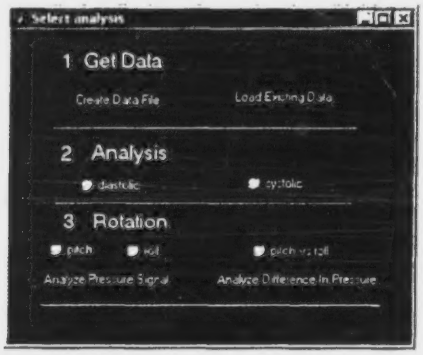

Fig. 9 Window 'Select analysis'.

STEP 7.1

In part 2 (Analysis), the user can select the pressure signal to be analyzed (systolic/diastolic). Unlike the classical option of system modeling, the advanced analysis considers the overall tilt scenario (HU-HD) and generates a discrete-time model for the corresponding pressure signal. Therefore, in part 3 (rotation), the user can select pitch, roll, or pitch vs. roll (to analyze the otolith response for a specific subject).

For example, in the above window we can choose to load subject *bc150 .mat* file previously created in step 4.0. We choose *systolic* pressure signal and we can analyze the *pitch* orientation signal as shown below.

When all indices (points) of interest are selected from the signal, the user can select the **Enter** option. The complete spline curve generated by interpolation between selected points will be displayed in blue as shown below.

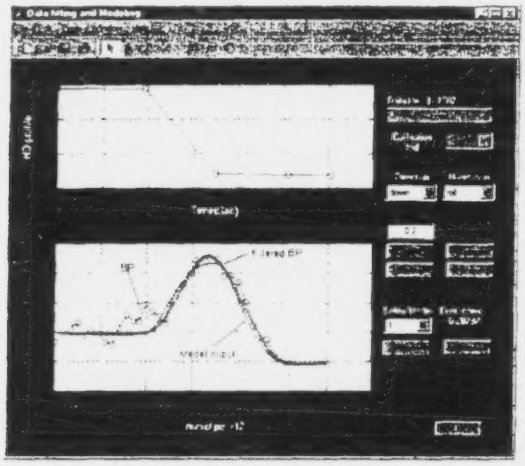

Fig. 8 Model output.

The blue curve generated above represents the filtered blood pressure signal without noise and outliers. Only meaningful pressure indices are picked by user and a smooth curve is fitted into them. To view the discrete-time second order model that represents the filtered blood pressure signal, the user has to first select the model prediction delay (default =1). The user can then click view and the model fit will be displayed in (light blue) as shown in the figure below. The sum of squared errors of the model vs. the filtered signal will also be displayed next to the model delay edit button..

If the model fit is not satisfactory, the user can relocate (change) some selected points to correct the model fit. Otherwise, if the fit is satisfactory, the user can click save button to store the corresponding second-order model parameters. Such parameters are indices located by user on the actual signal, model damping coefficient, model natural frequency, output-input model gain, and discrete-time prediction delay.

STEP 7.0

If the **system modeling (advanced)** option is selected in the system identification drop-down menu in step 3.0, a **select analysis** window will appear as shown below. In part 1 (Get Data), the user can create a .mat data file in a procedure identical to that in step 5.0. Otherwise, the user can load an existing .mat file that was generated on a previous system identification analysis run.

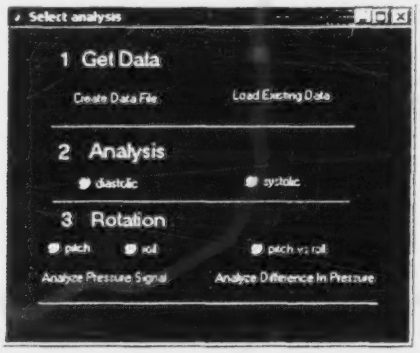

Fig. 9 Window 'Select analysis'.

STEP 7.1

In part 2 (Analysis), the user can select the pressure signal to be analyzed (systolic/diastolic). Unlike the classical option of system modeling, the advanced analysis considers the overall tilt scenario (HU-HD) and generates a discrete-time model for the corresponding pressure signal. Therefore, in part 3 (rotation), the user can select pitch, roll, or pitch vs. roll (to analyze the otolith response for a specific subject).

For example, in the above window we can choose to load subject *bc150 .mat* file previously created in step 4.0. We choose *systolic* pressure signal and we can analyze the *pitch* orientation signal as shown below.

Fig. 10 Window 'Select analysis'.

STEP 7.2

Once the above selection is made, the user can click the Analyze Pressure Signal button to start the system modeling analysis. The **system identification** options window shown below will be displayed.

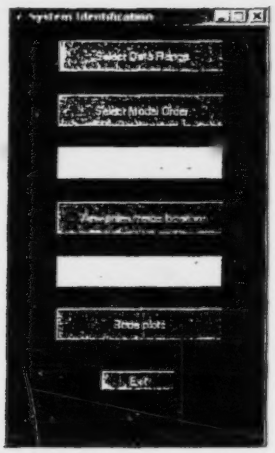

Fig. 11 Window 'System Identification'.

In the current window, step A involves the selection of the range for the data to be analyzed. In our example, when such option is selected, the pressure signal and corresponding tilt profile will be displayed as shown in the figure below. The minimum and maximum points on the blood pressure signal can be selected (for the current example 3, and 62 respectively). Once the range is specified the user can select **continue** button to model the selected portion of the signal.

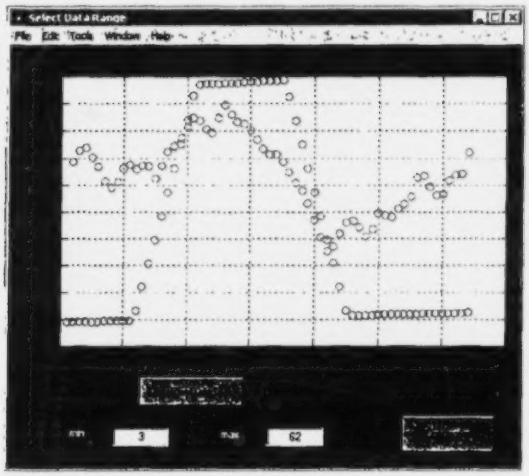

Fig. 12 Window 'Select Data Range'.

STEP 7.3

In the system identification options window, option B can now be chosen to automatically select a discrete-time model order that identifies the selected signal. When option B is chosen, the model order window shown below will be displayed. The suitable model order can be identified using least squares fit by pushing **Suitable OE order** button. The suitable model order bar on the figure will appear in red (second-order for the example adopted herein). Such selected order can be inputted in the **select order** edit box shown below otherwise the user can type in a different order (between 2 and 10). Once the model order is specified, we click next to view different structures of discrete-time models.

Fig. 10 Window 'Select analysis'.

STEP 7.2

Once the above selection is made, the user can click the Analyze Pressure Signal button to start the system modeling analysis. The **system identification** options window shown below will be displayed.

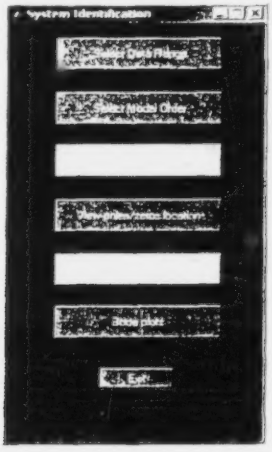

Fig. 11 Window 'System Identification'.

In the current window, step A involves the selection of the range for the data to be analyzed. In our example, when such option is selected, the pressure signal and corresponding tilt profile will be displayed as shown in the figure below. The minimum and maximum points on the blood pressure signal can be selected (for the current example 3, and 62 respectively). Once the range is specified the user can select **continue** button to model the selected portion of the signal.

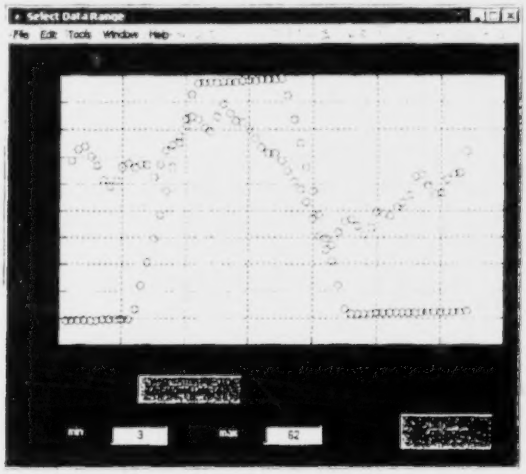

Fig. 12 Window 'Select Data Range'.

STEP 7.3

In the system identification options window, option B can now be chosen to automatically select a discrete-time model order that identifies the selected signal. When option B is chosen, the model order window shown below will be displayed. The suitable model order can be identified using least squares fit by pushing **Suitable OE order** button. The suitable model order bar on the figure will appear in red (second-order for the example adopted herein). Such selected order can be inputted in the **select order** edit box shown below otherwise the user can type in a different order (between 2 and 10). Once the model order is specified, we click next to view different structures of discrete-time models.

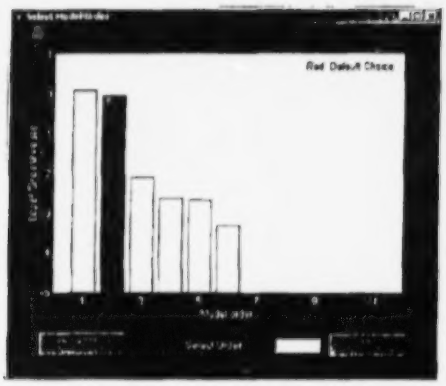

Fig. 13 Window 'Select Model Order'.

STEP 7.4

In the system identification option window, the next step would be option c (to view various model structures). When option c is chosen, the view model window shown below will be displayed.

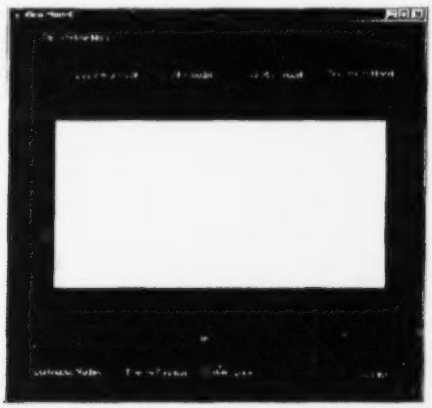

Fig. 14 Window 'View Model'.

The user can start by selecting the default Output error model structure fit. Then various model structures fit (ARX, ARMAX, Box-Jenkins) can also be displayed when their corresponding buttons are selected.

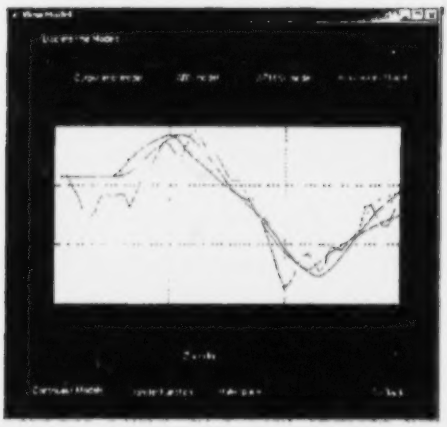

Fig. 15 Window 'View Model'.

STEP 7.5

Once the selected model structures are displayed, the user can select his model of choice by clicking on its corresponding icon. In this example, we selected the OE model structure (blue) as the most suitable representation for the pressure signal (magenta). The model transfer function and state-space parameters can be displayed on the Matlab command window by simply clicking the **Transfer Function** and **State space** icons.

After the model is identified, the user can choose the **Go back** option to return to the system identification option window in step 7.2. Option D in such a window displays the poles/zeros locations of the model identified in the above window. As shown below Options E and F display the step response, and the frequency-domain response of the model respectively.

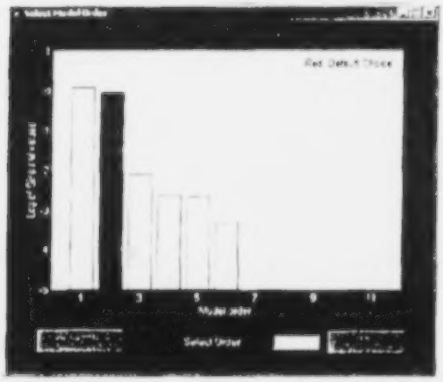

Fig. 13 Window 'Select Model Order'.

STEP 7.4

In the system identification option window, the next step would be option c (to view various model structures). When option c is chosen, the view model window shown below will be displayed.

Fig. 14 Window 'View Model'.

The user can start by selecting the default Output error model structure fit. Then various model structures fit (ARX, ARMAX, Box-Jenkins) can also be displayed when their corresponding buttons are selected.

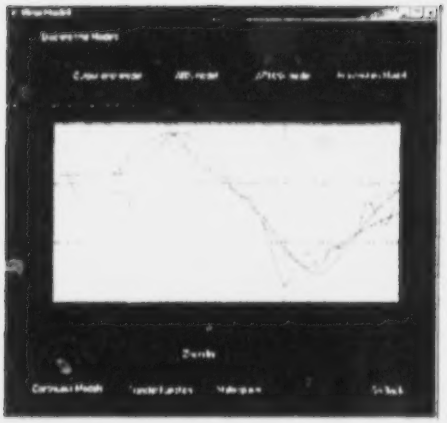

Fig. 15 Window 'View Model'.

STEP 7.5

Once the selected model structures are displayed, the user can select his model of choice by clicking on its corresponding icon. In this example, we selected the OE model structure (blue) as the most suitable representation for the pressure signal (magenta). The model transfer function and state-space parameters can be displayed on the Matlab command window by simply clicking the **Transfer Function** and **State space** icons.

After the model is identified, the user can choose the **Go back** option to return to the system identification option window in step 7.2. Option D in such a window displays the poles/zeros locations of the model identified in the above window. As shown below Options E and F display the step response, and the frequency-domain response of the model respectively.

Fig. 16 Window Step diagram and Roll Data

STEP 7.6

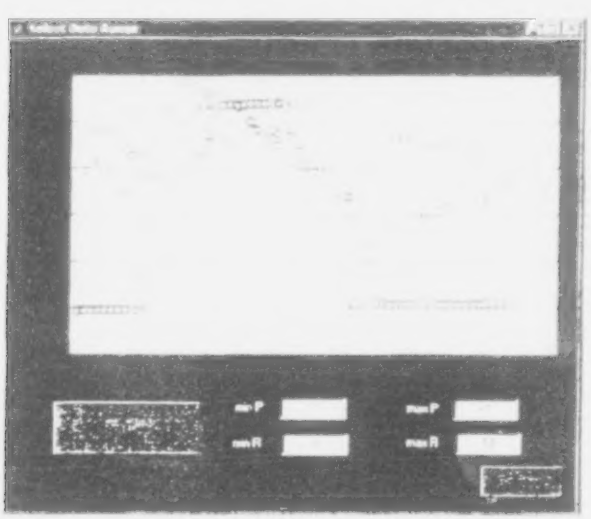

P517312 PDF [Page: 26 of 77]

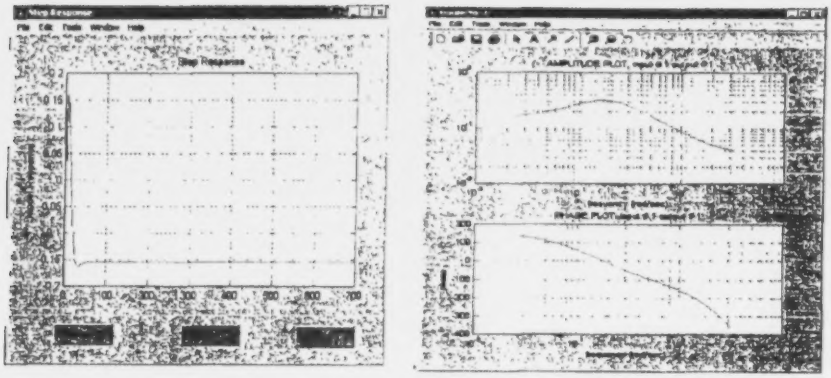

Fig. 16 Window 'Step Response and Bode Plot'.

STEP 7.6

In the data selection window in step 7.1, the user can also analyze the otolith response by simply checking **pitch vs. roll**. The analyze difference in pressure signal button will take the user to a window similar to options window in step 7.2. When the **select data range** button is selected, both the pitch and roll pressure signals (for the tilt scenario) will be displayed. The user can select the start/end points for each orientation type to ensure both signals are synchronized and have the same length (see example below).

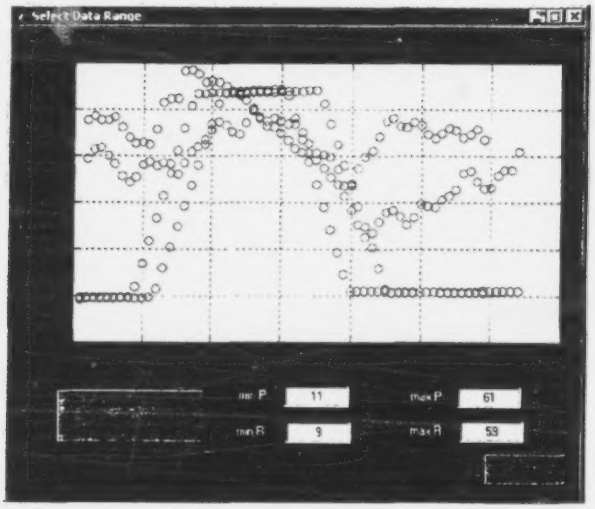

Fig. 17 Window 'Select Data Range'.

When the synchronization process is complete, the otolith response will be automatically identified by subtracting the pitch signal from the roll signal. The user can choose the Go Back button to further analyze such signal. The analysis procedure is identical to that performed in steps 7.3 – 7.5.

STEP 8.0

If the user selects the fuzzy modeling option in the system identification toolbox window in step 3.0, the modeling window shown below will be displayed. The window is split into two parts; (i) singleton input inference, and (ii) tilt scenario inference. The singleton input inference option allows the user to identify a split maneuvers from a drop-down menu ((i) HD pitch/ HU pitch, (ii) HD roll/ HU roll, (iii) HD pitch/ HU roll, and (iv) HD roll/ HU pitch), an arbitrary tilt rate, and an arbitrary dwell time as inputs. The outputs are approximations of various pressure indices (initial status, maximum drop, final status, overall drop from initial status, etc.) for the given inputs. For example, if we choose a HD roll/ HU pitch maneuver, a dwell time of 12 seconds, and a tilt rate of 35 deg/sec, we can infer the corresponding pressure indices and their time stamps for such a scenario as shown below. The values of the indices inferred below can be used in a generic sense to predict the response of various subjects when the tilt profile and orientation specified below are applied in a maneuver.

Table 2. Fuzzy Model Inputs and Outputs.

Inputs:			Outputs				
Orientation: PTP RTR PTR RTP	Dwell time (sec) (7 ~ 30)	Rate (deg/sec) (15 ~ 45)	Initial status (mm Hg)	Maximum drop (mm Hg)	Time of maximum drop (sec)	Final status (mm Hg)	Recovering time (sec)

P517312.PDF [Page: 28 of 77]

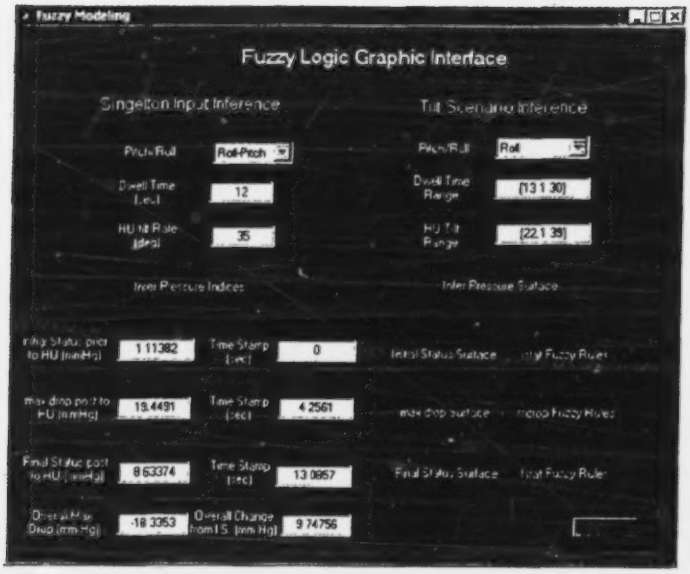

The tilt scenario inference option allows the user to select an orientation (pitch/roll) from a drop-down menu, a range for the dwell time, and a range for the tilt rate as inputs (as shown on the R.H.S of the above figure). It displayed various pressure surfaces that represent the variation of different indices (initial status, maximum drop, and final status) for the input ranges specified. For example, under roll orientation, the dwell time is selected between 13 and 30 (INPUT1) and the tilt rate is selected between 22 and 39 (INPUT2). The **infer pressure surface** button can be used to display surfaces that shows the variation of pressure indices for the inputs ranges specified. In the figures below, we choose to display the initial status surface and its corresponding rules, the maximum drop surface and its corresponding rules, and the final status surface and its corresponding rules.

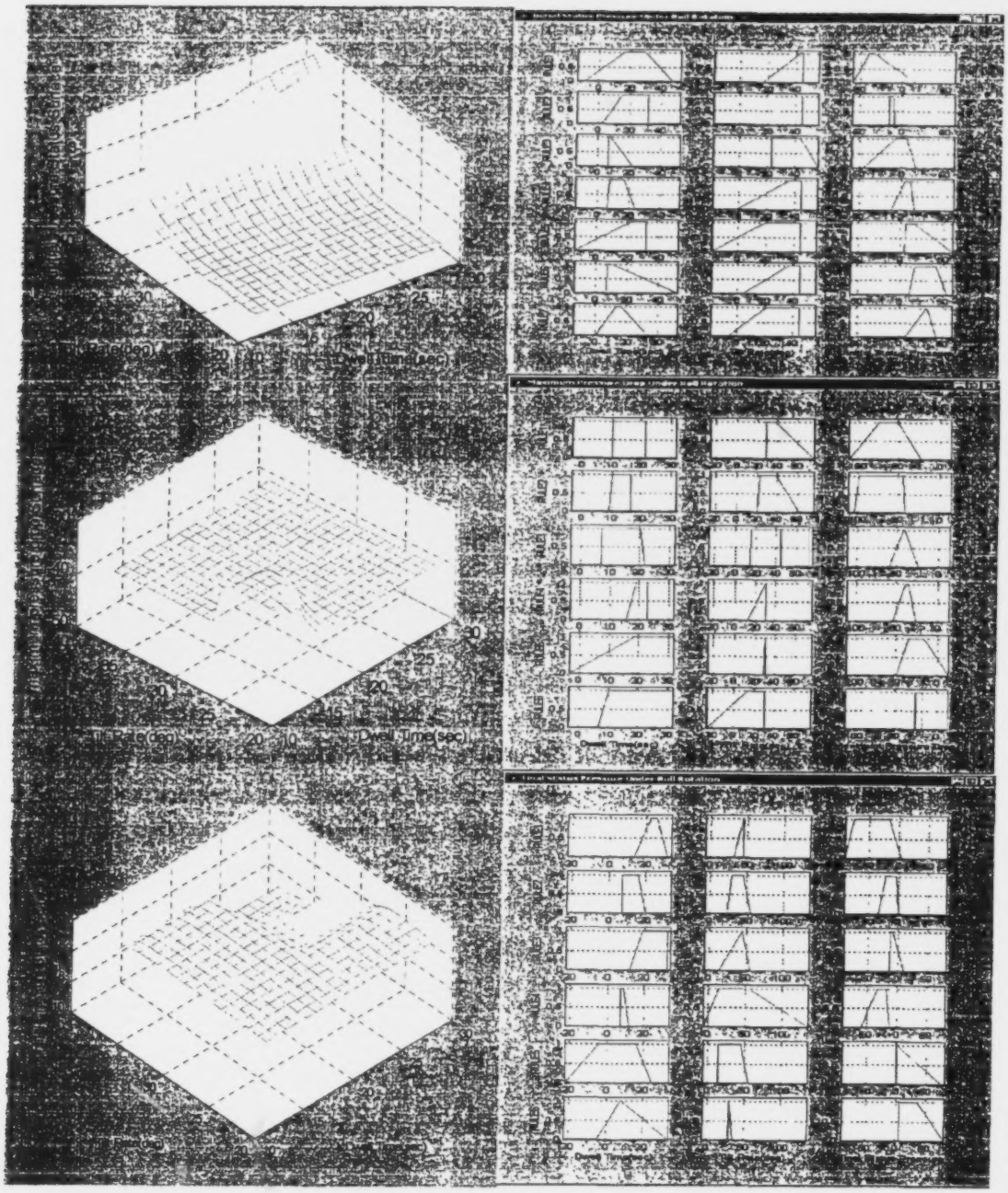

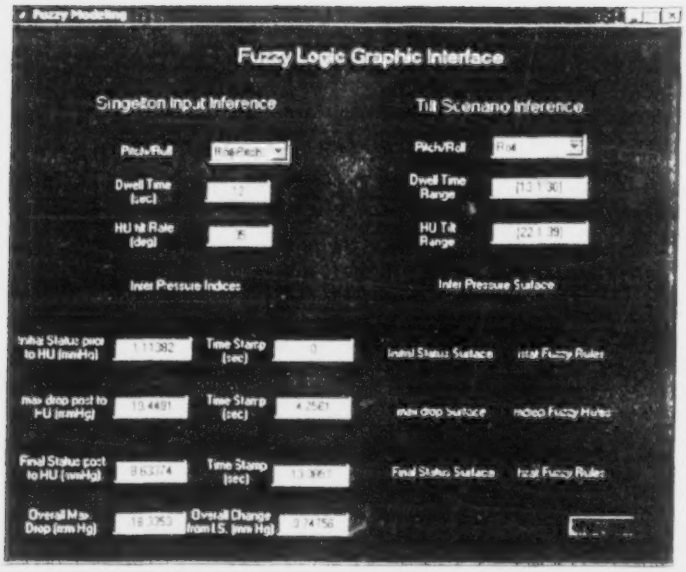
Fuzzy Modeling
Fuzzy Logic Graphic Interface
Singelton Input Inference
Pitch/Roll
Dwell Time (sec)
HU tilt Rate (deg)
Infer Pressure Indices
Initial Status prior to HU (mmHg)
Time Stamp (sec)
max drop post to HU (mmHg)
Time Stamp (sec)
Final Status post to HU (mmHg)
Time Stamp (sec)
Overall Max Drop (mm Hg)
Overall Change from I.S. (mm Hg)
Tilt Scenario Inference
Pitch/Roll
Dwell Time Range
HU Tilt Range
Infer Pressure Surface
Initial Status Surface
Initial Fuzzy Rules
max drop surface
mdrop Fuzzy Rules
Final Status Surface
final Fuzzy Rules

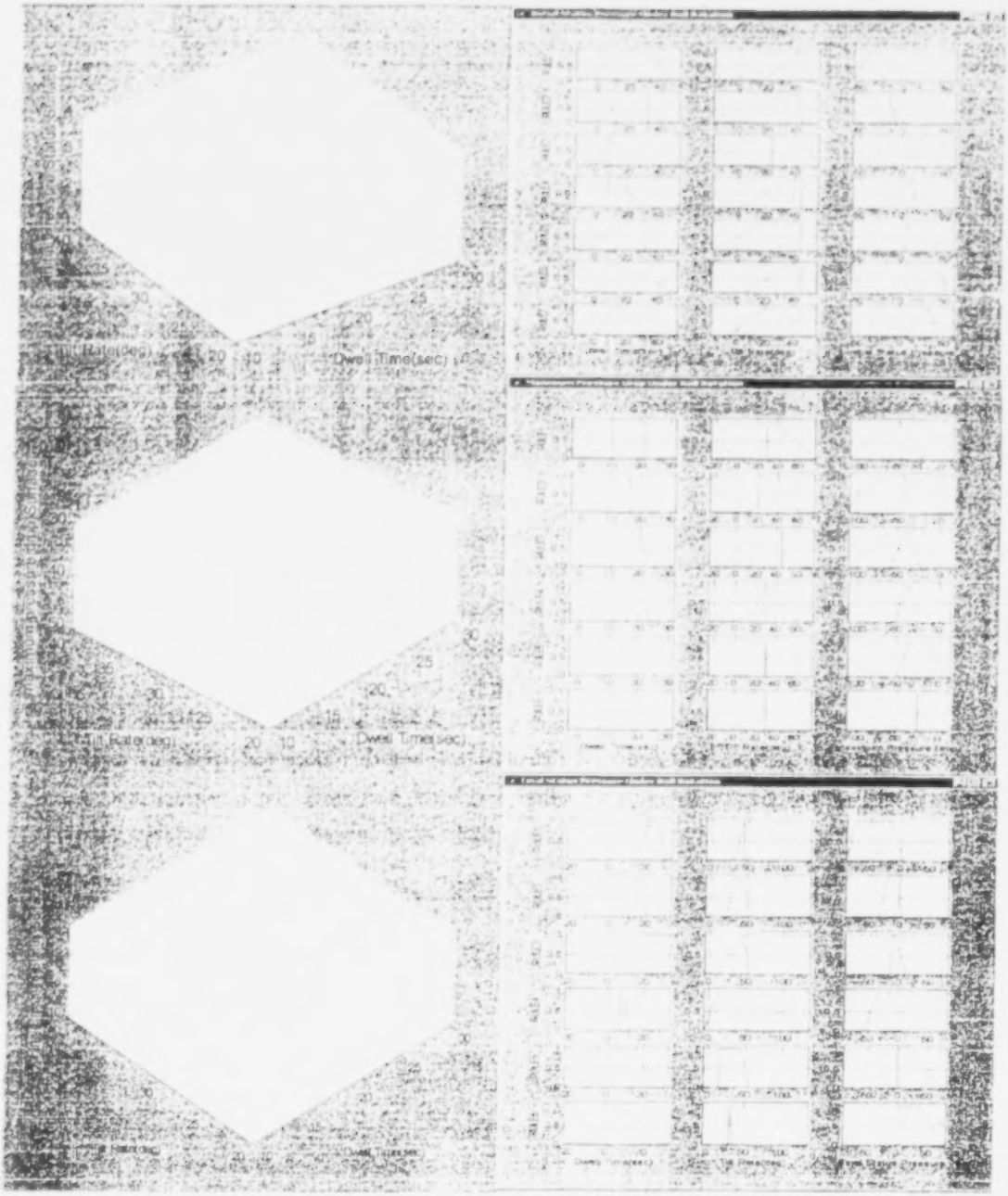

STEP 9.0

For the CROST Toolbox window in Step 2.0, the user has the option to perform statistical analysis on raw data obtained from experiments. Such option can be selected by a left-click on the statistical analysis icon. The window below will appear. The user has the option to input subject's information by choosing the setup option in this window. The procedure is identical to that in step 4.0.

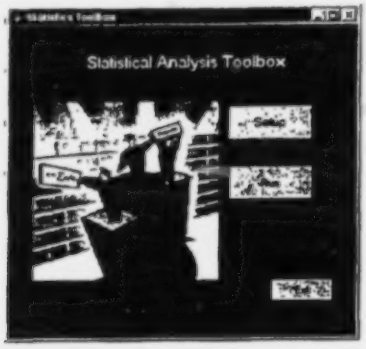

To perform statistical analysis on raw data, the user will choose the run option from the above window. Such selection will open the statistical analysis options window shown below. Analysis methods include paired t-tests, permutation tests, one/two way ANOVA tests, and linear regression analysis.

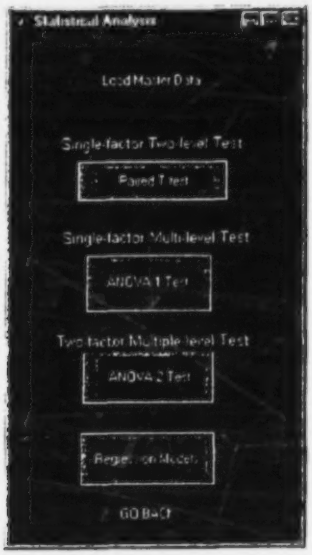

The statistical analysis starts with a "load data" procedure. Such a procedure is applied to a master document (defined by the user) to extracts factors and indices to be analyzed. An example

of a master document is shown below. It includes subjects names, and numbers. The factors of intersect in the example file below are orientation (1:pitch, 2:roll), tilt rate, and dwell time. The pressure indices are defined as initial status, maximum drop and its time stamp (MDT), and final status and its time stamp (FST). Such file can be saved as a text or data file.

Subject	SI	Orientation	Rate	DwellTime	InitStatus	MaxDrop	MDT	FinalStatus	FST
Fr	2	1	45	76	-1	-170	62	02	154
Fr	2	2	45	91	19	-406	58	00	169
Ivan	3	1	45	73	-4	-269	88	-86	182
Ivan	3	2	45	74	22	-340	88	-224	151
Jim	4	1	45	71	-10	-182	56	166	203
Jim	4	2	45	88	-5	-315	40	35	202
Kevin	5	1	45	94	15	-257	20	-202	38
Kevin	5	2	45	110	14	-277	40	-62	938
Lg	6	1	45	75	-4	-294	48	-39	168
Lg	6	2	45	78	8	-372	42	22	15
Mb	7	1	45	67	-6	00	00	63	135
Mb	7	2	45	80	-2	-301	30	-87	13
Pt	8	1	45	85	11	-321	58	-308	32
Pt	8	2	45	81	17	-490	28	-226	9
Ted	9	1	45	75	-10	-199	60	37	212
Ted	9	2	45	76	20	-451	70	-347	108

When the user selects the load data for statistical analysis, the explorer window will open to allow the user to select a master document similar of a form similar to the file given above. If the file is chosen successfully, the select indices window shown below will appear to allow the user to select specific factors and indices columns for statistical analysis.

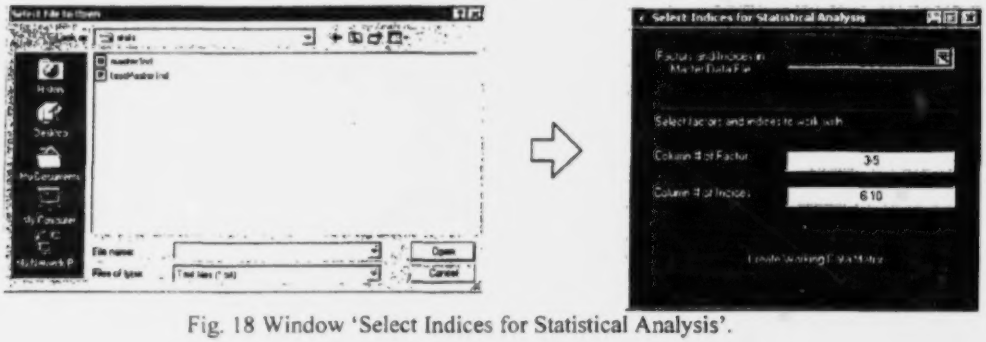

Fig. 18 Window 'Select Indices for Statistical Analysis'.

In the indices selection window, the user can specify the column numbers for both factors and indices. For example, if we select columns 3:5 in the factors window, we select orientation, dwell

STEP 9.0

For the CROST Toolbox window in Step 2.0, the user has the option to perform statistical analysis on raw data obtained from experiments. Such option can be selected by a left-click on the statistical analysis icon. The window below will appear. The user has the option to input subject's information by choosing the setup option in this window. The procedure is identical to that in step 4.0.

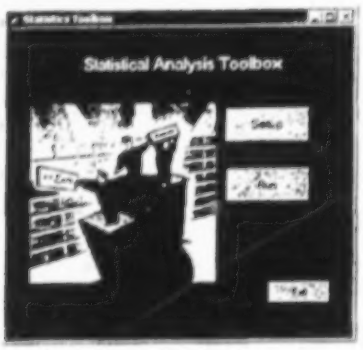

To perform statistical analysis on raw data, the user will choose the run option from the above window. Such selection will open the statistical analysis options window shown below. Analysis methods include paired t-tests, permutation tests, one/two way ANOVA tests, and linear regression analysis.

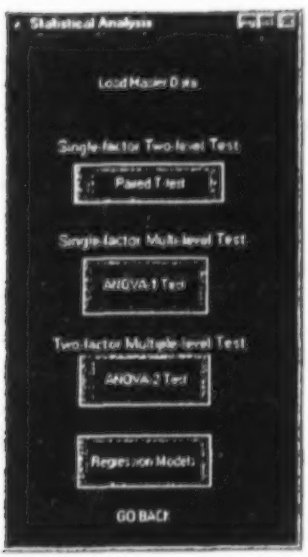

The statistical analysis starts with a "load data" procedure. Such a procedure is applied to a master document (defined by the user) to extracts factors and indices to be analyzed. An example

of a master document is shown below. It includes subjects names, and numbers. The factors of intersect in the example file below are orientation (1:pitch, 2:roll), tilt rate, and dwell time. The pressure indices are defined as initial status, maximum drop and its time stamp (MDT), and final status and its time stamp (FST). Such file can be saved as a text or data file.

Subject	SI	Orientation	Rate	DwellTime	IniStatus	MaxDrop	MDT	FinalStatus	FST
Fr	2	1	45	7.6	3	-17.0	6.2	0.2	15.4
Fr	2	2	45	9.1	19	-40.6	5.8	0.3	16.4
Ivan	3	1	45	7.3	-4	-26.9	8.5	-8.5	18.2
Ivan	3	2	45	7.4	22	-34.0	8.8	-22.4	19.1
Jim	4	1	45	7.1	-16	-18.2	5.6	16.6	20.3
Jim	4	2	45	8.8	5	-31.5	4.0	3.5	20.2
Kevin	5	1	45	9.4	35	-25.7	2.0	-20.2	3.8
Kevin	5	2	45	11.0	14	-27.7	4.0	-6.2	9.38
Lg	6	1	45	7.5	4	-29.4	4.8	-3.9	16.8
Lg	6	2	45	7.8	8	-37.2	4.2	2.2	18
Mb	7	1	45	6.7	-6	0.0	0.0	6.3	13.5
Mb	7	2	45	8.0	-2	-30.1	3.0	-8.7	13
Pr	8	1	45	8.5	11	-32.1	5.8	-30.8	3.2
Pr	8	2	45	8.1	17	-49.0	2.8	-22.6	9
Ted	9	1	45	7.5	10	-19.9	6.0	3.7	21.2
Ted	9	2	45	7.6	20	-45.1	7.0	-34.7	10.8

When the user selects the load data for statistical analysis, the explorer window will open to allow the user to select a master document similar of a form similar to the file given above. If the file is chosen successfully, the select indices window shown below will appear to allow the user to select specific factors and indices columns for statistical analysis.

Fig. 18 Window 'Select Indices for Statistical Analysis'.

In the indices selection window, the user can specify the column numbers for both factors and indices. For example, if we select columns 3:5 in the factors window, we select orientation, dwell

time, and tilt rate from our sample master document. Also, if we select columns 6:10 for indices, then we select initial status, maximum drop and its time stamp (MDT), and final status and its time stamp (FST).

The factors and indices selected can be used to create a so-called working data matrix by simply clicking the corresponding push button. Now we are ready to analyze the selected data matrix.

From the statistical analysis options window, if paired t-tests are to be performed, a click on the corresponding icon will display the window shown below. In the group menu, the user has to choose the column number he wishes to create (1 or 2). In the measurement for group data drop-down menu, the user has to specify the index of blood pressure to be analyzed for every column. In the factor menu, the user has to pick every factor and then input its range of interest in the corresponding factor level edit box.

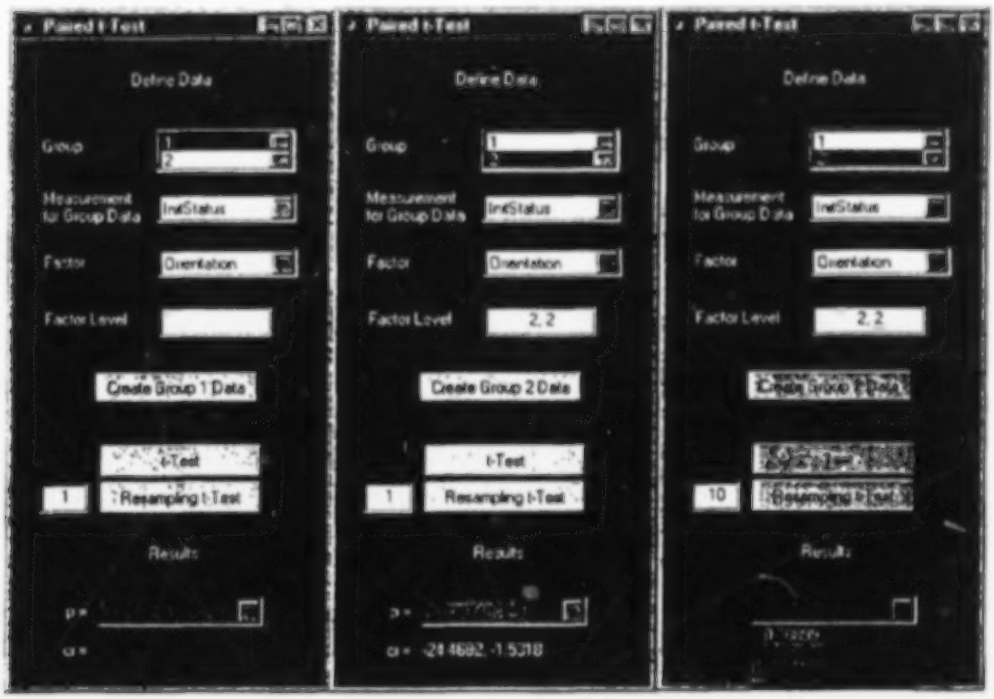

Fig. 19 Window 'Paired t-Test', before, after performing t-Test and re-sampling t-Test.

For every column, the user has the option to view the corresponding group data in the form of a box plot that would allow for filtering outliers in the generated index data. Such option is selected from the above window by choosing the **view Group () Data** option. The window that allows the user to filter outliers is shown below.

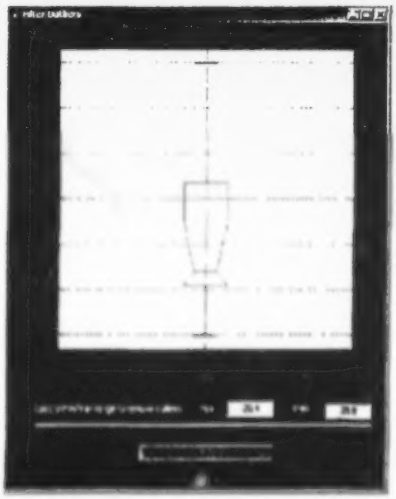

After the user specifies the minimum and maximum range in the group to reject the outliers, a click on the back button will take the user to the paired t-test window again to generate group data for column 2 in a similar fashion. When both columns are created, the user can select the t-test icon to view the results of the analysis. The results of the t-test hypothesis (the means of both columns are equal), significance, and confidence intervals will be displayed in the same window in Fig. 19.

The statistical toolbox also provides one-way and two-way ANOVA tests and Linear Regression Model. For paired t-Test and one-way ANOVA, the re-sampling using 'bootstrap' method is also provided in the toolbox for non-parametric testing. The following figures show examples of these tests.

Table 3. Example of one-way ANOVA test

Group 1 data	Group 2 data	P value
Pitch, rate = 45, dwell time = 30	Roll, rate = 45, dwell time = 30	0.024

time, and tilt rate from our sample master document. Also, if we select columns 6:10 for indices, then we select initial status, maximum drop and its time stamp (MDT), and final status and its time stamp (FST).

The factors and indices selected can be used to create a so-called working data matrix by simply clicking the corresponding push button. Now we are ready to analyze the selected data matrix.

From the statistical analysis options window, if paired t-tests are to be performed, a click on the corresponding icon will display the window shown below. In the group menu, the user has to choose the column number he wishes to create (1 or 2). In the measurement for group data drop-down menu, the user has to specify the index of blood pressure to be analyzed for every column. In the factor menu, the user has to pick every factor and then input its range of interest in the corresponding factor level edit box.

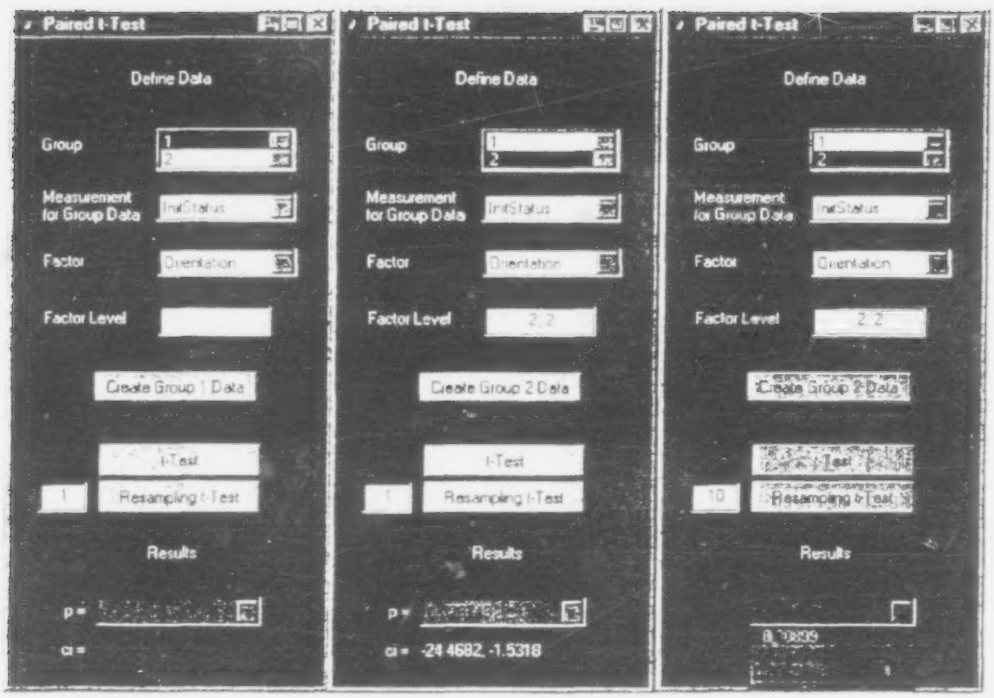

Fig. 19 Window 'Paired t-Test', before, after performing t-Test and re-sampling t-Test.

For every column, the user has the option to view the corresponding group data in the form of a box plot that would allow for filtering outliers in the generated index data. Such option is selected from the above window by choosing the **view Group () Data** option. The window that allows the user to filter outliers is shown below.

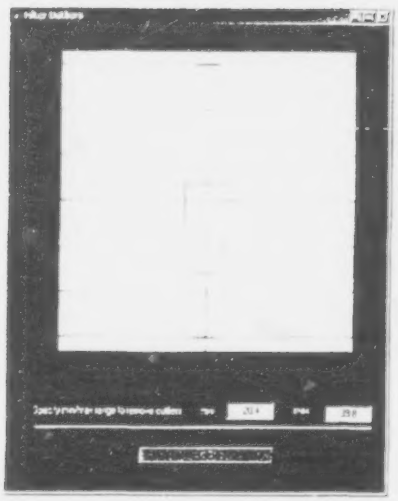

After the user specifies the minimum and maximum range in the group to reject the outliers, a click on the back button will take the user to the paired t-test window again to generate group data for column 2 in a similar fashion. When both columns are created, the user can select the t-test icon to view the results of the analysis. The results of the t-test hypothesis (the means of both columns are equal), significance, and confidence intervals will be displayed in the same window in Fig. 19.

The statistical toolbox also provides one-way and two-way ANOVA tests and Linear Regression Model. For paired t-Test and one-way ANOVA, the re-sampling using 'bootstrap' method is also provided in the toolbox for non-parametric testing. The following figures show examples of these tests.

Table 3. Example of one-way ANOVA test

Group 1 data	Group 2 data	P value
Pitch, rate = 45, dwell time = 30	Roll, rate = 45, dwell time = 30	0.024

P517312.PDF [Page: 34 of 77]

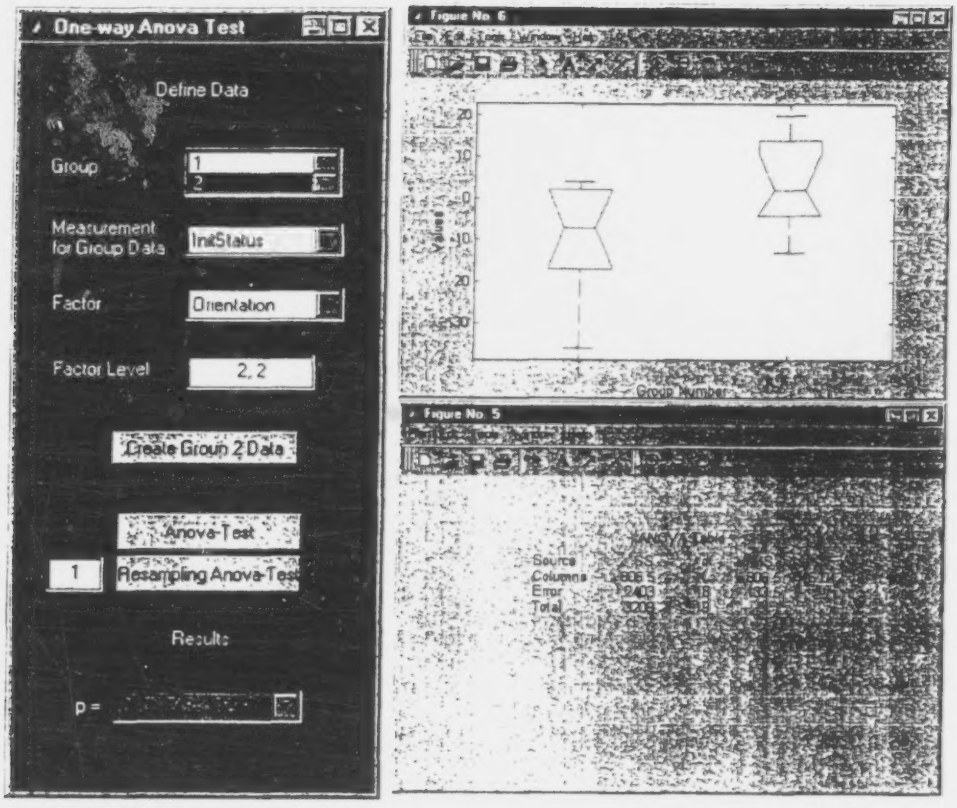

Fig. 20 Windows for one-way ANOVA test.

Table 4. Example of two-way ANOVA test (Rate = 45)

	Factor 1 (orientation)	Factor 2 (dwell time)	P value
Level 1	Pitch	7	P1 = 0.00004
Level 2	Roll	15	P2 = 0.0003
Level 3		30	P1,2 = 0.95

P517312.PDF [Page: 35 of 77]

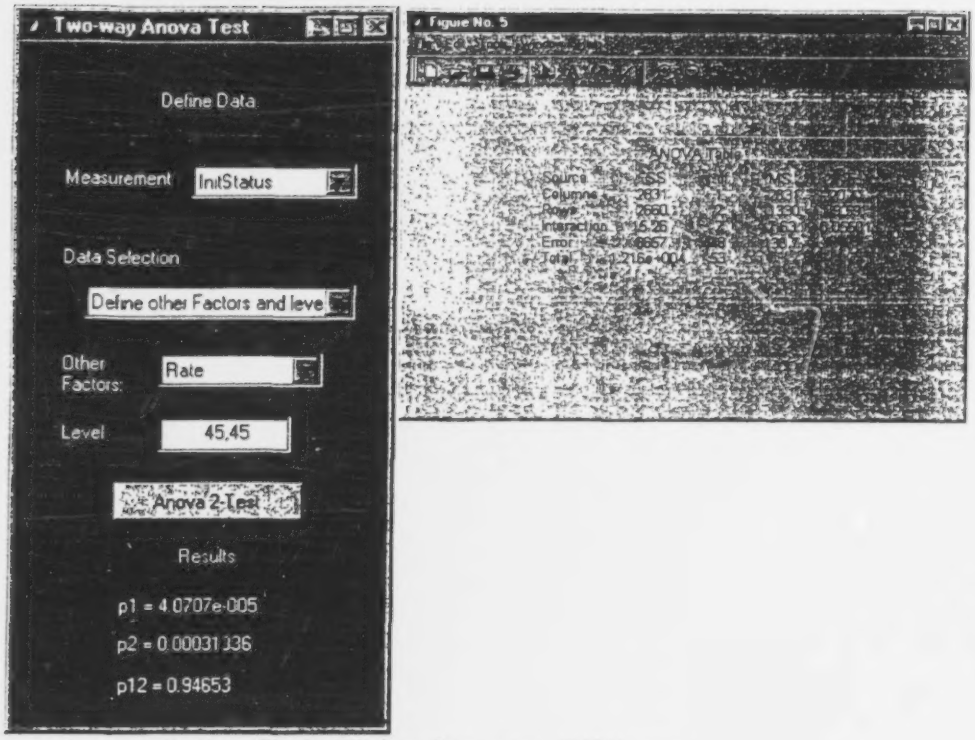

Fig. 21 Windows for two-way ANOVA test.

Table 5. Example of Linear Regression Model (Rate = 45)

	Factor 1 (orientation)	Factor 2 (dwell time)	Factor 3 (rate)
Range	Pitch and roll	7 ~ 30	15 ~ 45

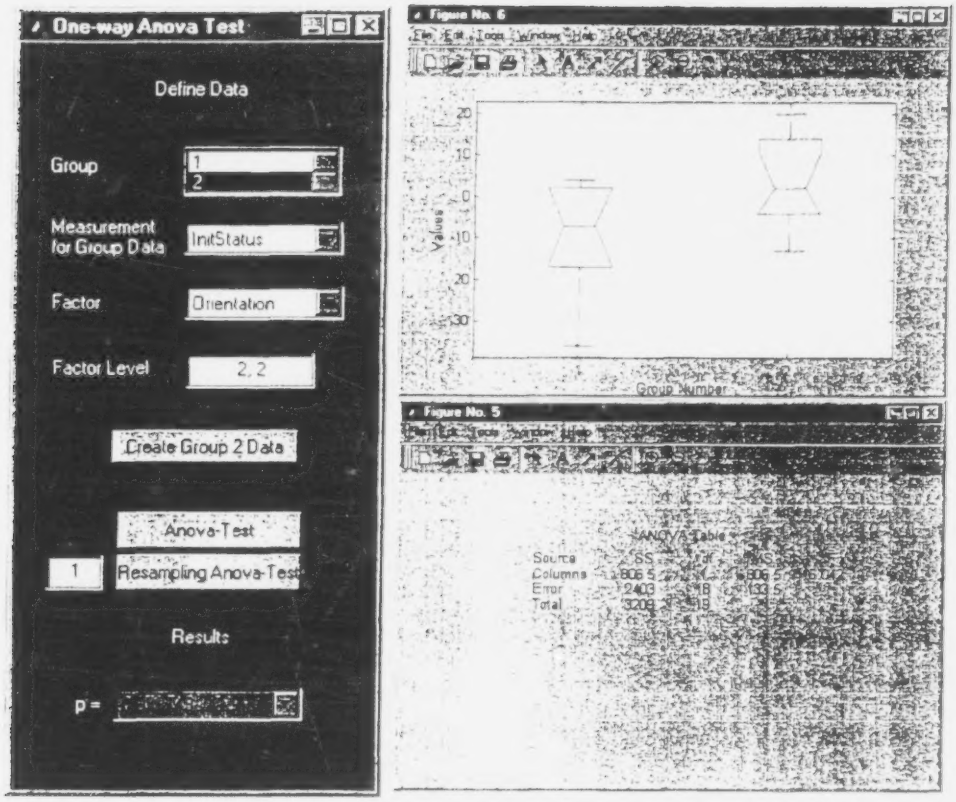

Fig. 20 Windows for one-way ANOVA test.

Table 4 Example of two-way ANOVA test (Rate = 45)

	Factor 1 (orientation)	Factor 2 (dwell time)	P value
Level 1	Pitch	7	P1 = 0.00004
Level 2	Roll	15	P2 = 0.0003
Level 3		30	P1,2 = 0.95

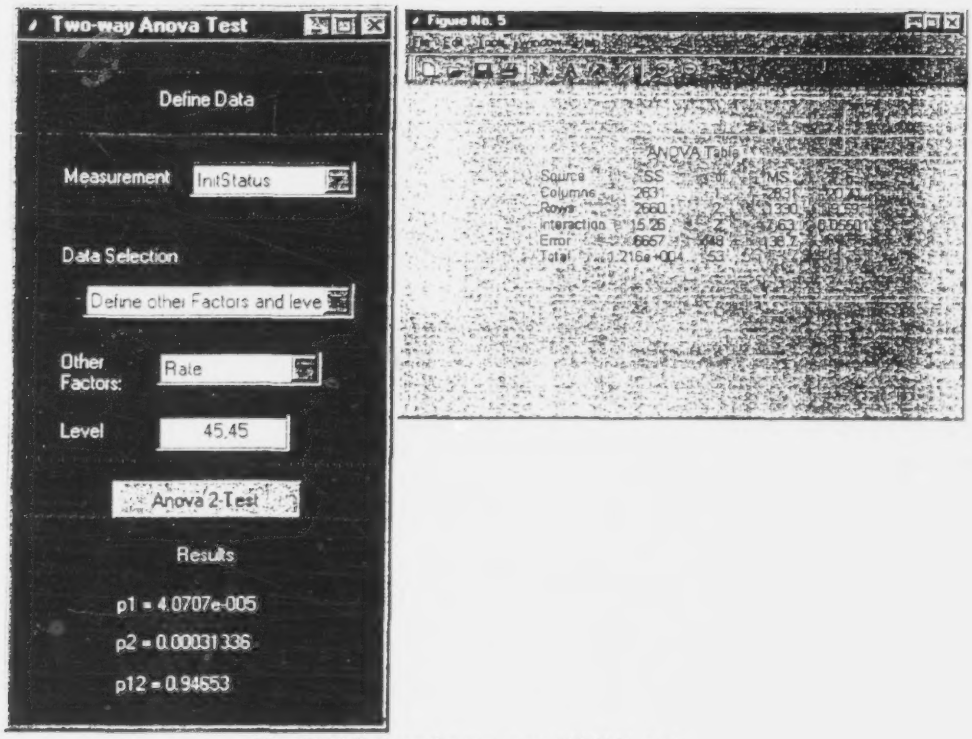

Fig. 21 Windows for two-way ANOVA test.

Table 5. Example of Linear Regression Model (Rate = 45)

	Factor 1 (orientation)	Factor 2 (dwell time)	Factor 3 (rate)
Range	Pitch and roll	7 ~ 30	15 ~ 45

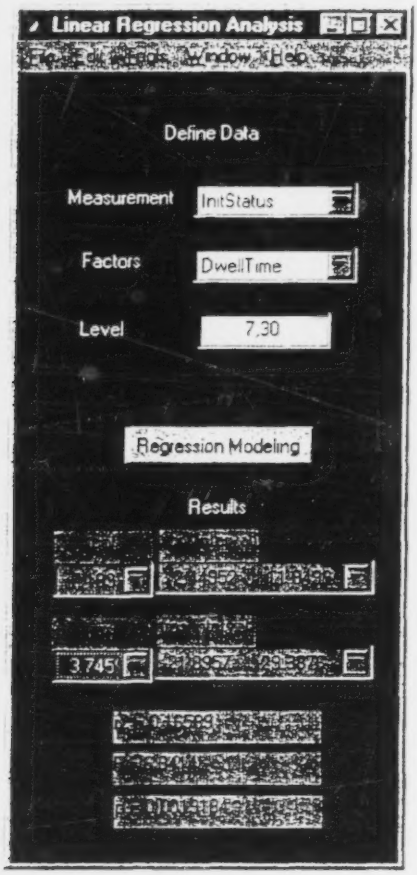

Fig. 21 Windows for Linear Regression Model test.

P517312.PDF [Page: 36 of 77]

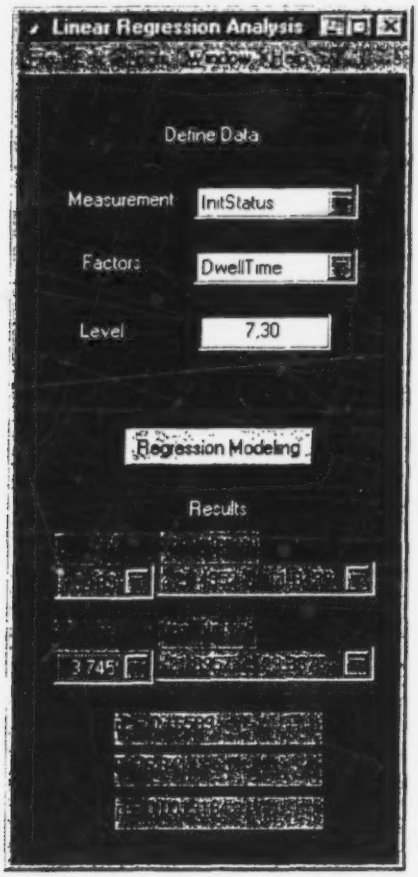

Fig. 21 Windows for Linear Regression Model test.

P517312.PDF [Page: 37 of 77]

Modeling of Dynamic Cardiovascular Responses During G-transition Induced Orthostatic Stress in Pitch and Roll Rotations

William W. Melek*, Ziren Lu*, Alex Kapps*, Bob Cheung**

* *Engineering Services Inc. (ESI), 1 Bedford Road, Unit 5, Toronto, Ontario, Canada, M5R 2J7*
** *Defence and Civil Institute of Environmental Medicine (DCIEM), 1133 Sheppard Avenue West, Toronto, Ontario, Canada, M3M 3B9*

ABSTRACT

Dynamic and fuzzy models for a typical subject's cardiovascular response to the orthostatic stress have been developed based on experimental data. In our original study [1], arterial blood pressure time-series data were obtained using a man-rated tilt table that applies Gz-acceleration transitions from +0.861 Gz (HU) to – 0.707 G (HD) and back to +0.861 Gz (HU) using either pitch or roll rotations [1]. G transitions of different duration and onset rates are common in fighter maneuvers. Based on these data, two types of predictive models have been developed in this paper: **(i)** second-order discrete-time models that predict blood pressure dynamics during pitch and roll rotations; and **(ii)** fuzzy logic models that predict important variations in a subject's cardiovascular dynamics induced by HU-to-HD and HD-to-HU transitions. These two types of models assist in providing an operationally important predictive view on the characteristics of blood pressure responses to orthostatic stress induced by pitch and roll rotations of a fighter jet pilot. The new models are being currently utilized in the design of operational recommendations for more G-tolerant operational flight regimes (e.g., split-S tactical maneuver) for modern combat aircraft than the ones currently in use.

1. Introduction

As early as 1953, von Beckh reported that during in-flight research, alternating hypogravity (Gz<1G) and hypergravity (Gz>1G) resulted in decreases in G-tolerance and in the efficiency of physiological recovery ([10], [2]). Other evidence, such as in-flight

study [11], a centrifuge investigation [12], and an anecdotal report [13] have also indicated that there exists a definite deleterious effect on +Gz tolerance when a pilot is subjected to the transition of negative to positive Gz. A recent survey by the USAF indicated that maneuvers of G-transition ranging from 0 to +0.5 Gz for 3.5 to 5s are common in air combat training missions [14]. Moreover, in a fighter aircraft, one of the common methods used to acquire tactical advantage over the opponent is the Split-S maneuver, which involves "unloading" the aircraft prior to accelerating. With few exceptions, this maneuver involves rolling and pulling all the G aerodynamically available. The effects of point roll or unloaded barrel roll maneuver on cardiovascular response to the subsequent increase in the acceleration needs to be investigated.

Our previous study [1] was designed to investigate arterial pressure changes under orthostatic stress in either pitch or roll rotations by exposing subjects to head-up (HU, 1G) to head-down (HD, <1G) and back to HU (1G) transitions using a tilt table. The tilt table used is shown in Figure 1. Figure 2 shows typical pitch and roll rotations considered in our study. The results of the current paper concur with the statistical analysis results presented in [1] and indicate that the human cardiovascular system might have different responses to orthostatic stress induced by the pitch and roll rotations.

In this paper, we develop dynamic models for the prediction of the arterial blood pressure time-series response under pitch and roll rotations. Analysis of these models have proven useful in exploring the behavior of the human's cardiovascular system in either pitch or roll rotation from HU to HD and then back from HD to HU under different experimental/flight conditions: (i) variable HD (i.e., hypogravity) dwell times; and (ii) variable tilt-table rotation rates that correspond to acceleration onset rates in fighter

aircraft. Finally, fuzzy models have been developed to predict the indices of arterial blood pressure response to the aforementioned experimental/operational conditions.

2. Second Order Modeling of Cardiovascular Responses

Eleven healthy volunteers participated in this study. All of the subjects had pervious experience with the tilt table. The man-rated electronic tilt table can accommodate either a seated or standing subject with a range of 15° (HU, G ≈ 0.86g) to 135° (HD, G ≈ -0.7g) tilt. Zero degree is considered to be the gravitational vertical. The angular velocity of the tilt table can be set from 5° s^{-1} to a maximum of 45° s^{-1} in 5° increments. A transducer attached to the tilt table records the tilt angle. A fingertip BP monitor was used for continuous measurement of systolic and diastolic BP. During each trial, the subject was positioned onto the tilt table with his feet secured to the foot support plate. In pitch orientation the subject faces forward with his back against the tilt table. In roll orientation the subject faces sideways with his shoulder against the tilt table. Fig. 3 shows typical systolic pressure measurements during a complete HU-HD-HU maneuver in pitch or roll orientation.

During the transition from HU to HD, the typical BP record increases sharply and reaches its maximum value in 2.5s. After that BP gradually decreases over the next 10s and then recovers slightly to a steady-state level for the remainder of the HD period. During the transition from HD to HU, BP immediately decreases to its lowest point in about 2s and then gradually increases to a steady level over the next 5~15s. In addition to this major pattern of changes in BP, there exist significant ripples in the BP signal that are caused by the factors such as breathing or other physiological actions.

P517312.PDF [Page: 40 of 77]

In general, each human's cardiovascular system is unique and quite nonlinear so that it behaves differently in different orientations and during different G transitions (HU to HD or HD to HU). Therefore, a set of dynamic models has initially been generated to model BP responses of each subject under different experimental conditions. To generalize across the population of test subjects, we have established, by using the appropriate system identification procedures, that a second-order dynamic model is optimal for modeling the dynamic BP time-series. The optimality requirements are: (i) a candidate model is to filters out the ripples and other secondary effects present in the blood pressure signal due to the breathing pattern and other effects unrelated to the actual G transition; and (ii) a candidate model remains stable and sufficiently sensitive for replicating the foremost changes of BP under G transitions for both pitch and roll rotations.

By analyzing all of the experimental data from different subjects, the output error (OE) model [3] was found to be superior over other models in terms of matching performance with actual BP responses. This model possesses the most flexible structure for modeling a subject's cardiovascular response, i.e., systolic and diastolic blood pressure signals. A general form of a discrete-time output error model is given as in [3]:

$$y(k) = \frac{B(q^{-1})}{F(q^{-1})} u(k-n) + e(k) \qquad \textbf{(1)}$$

where $y(k)$ is the system output, i.e., systolic or diastolic blood pressure. The model input $u(k)$ is the tilt angle dependent on the tilt rate and HD duration (i.e., dwell time) of a G-maneuver. The model disturbance is given by $e(k)$ and the sampling instance is given by k. Finally, the prediction delay operator is defined q^{-1}.

The overall BP data were divided into four groups: pitch or roll during HU-HD or HD-HU. As to the HU-HD phase, only those with HD dwell time of 30s were used for modeling since the HD BP dynamics typically settle down to a stable level after 15s. With respect to the HD-HU phase, it is further classified into sub-groups based on HD dwell time duration (7s, 15s, or 30s) and the tilt rate from HD to HU. For each group and subject a second order model is obtained. We have smoothened the BP data by removing ripples while keeping the valuable information in the signal intact. Fig. 4 and 5 show the models for a subject in pitch and roll rotations during HU-HD and HD-HU transitions.

After all the models for each subject were obtained, their parameters were averaged to obtain the statistical model correct across the population of test subjects for each combination of pith/roll rotations at different dwell times and offset rates. Fig 6 present the averaged pitch and roll model responses to HU-HD and HD-HU transitions with the dwell time of 30s and offset rate of $45^{o}s^{-1}$. Table 1 shows the model parameters.

The above models can be used to predict the averaged BP dynamics of pilots who undergo G transitions during operational flight maneuvers such as split-S maneuver shown in Figure 7. In addition to using these models, it will be advantageous to know in advance the variations in BP expressed in terms of carefully defined and practically (i.e., physiologically and operationally) significant indices, such as a subject's maximum drop in BP after the completion of a G transition. Other indices of interest are shown in Fig 9 and summarized in Table 2 below.

In an attempt to provide a model that is able to predict these indices based on the *a priory* known information about a typical flight maneuver (i.e., information on whether pitch or roll rotation is employed during a split-S or other maneuvers) and its corresponding G

P517312.PDF [Page: 42 of 77]

transition (parameterized according to the G level, dwell times and offset rates), fuzzy logic techniques have been employed. The details on the fuzzy modeling approach and models developed are provided in the next section.

3. Fuzzy-Logic Modeling

In line with the observation established in the previous section in regards to the variability of the human cardiovascular response in pitch or roll rotations, HD dwell times and offset rates, these experimental conditions have been defined as inputs to the modeling architecture that generates the appropriate fuzzy models of G-transition induced orthostatic stress. The cardiovascular response indices, such as *the maximum drop in BP following a HD-HU transition, the final status of blood pressure once the orthostatic stress is removed*, etc (see Fig 9 and Table 2) have been defined as the fuzzy model outputs. The outputs are shown schematically in Fig 9 for a typical blood pressure response. The first index, i.e., heart-level blood pressure drop in HD position is associated with the HU-HD G-transition profile. The second and third indices, i.e., maximum drop in BP following HD to HU transition and the final status of blood pressure are associated with HD-HU G-transition profile.

The fuzzy modeling approach can therefore infer the cardiovascular response indices given a tilt scenario (maneuver) represented by the tilt rotation type (pitch or roll), tilt rate and HD dwell time. Hence, we can predict the blood pressure response expressed by the characteristic indices in each of a "multiple" consecutive flight maneuvers (such as split-S maneuver) and G-transitions using a set of the fuzzy rules developed and the suitable inference mechanism embedded in software.

P5[7:1]2.PDF [Page: 43 of 77]

Fuzzy systems are based on the concept of fuzzy partitioning of information. The decision-making ability of the fuzzy model depends on the existence of a set of rules and a fuzzy reasoning mechanism. In general, the encoded knowledge of a Multi-Input Multi-Output (MIMO) system can be interpreted by fuzzy models consisting of IF-THEN rules with multi-antecedent and multi-consequent variables (with r antecedents, s consequents, and n rules) as shown in Fig 8. In this figure, $U_1, U_2, \ldots, U_r$ are input variables, and $V_1, V_2, \ldots, V_s$ are output variables, B_{ij} $(i=1,\ldots,n,\ j=1,\ldots,r)$ and D_{ik} $(i=1,\ldots,n,\ k=1,\ldots,s)$ are fuzzy sets of the universes of discourse $X_1, X_2, \ldots, X_r$ and $Y_1, Y_2, \ldots Y_s$ of $U_1, U_2, \ldots, U_r$ and $V_1, V_2, \ldots, V_s$, respectively.

A typical approach to fuzzy modeling involves two major steps: **(i)** a parameterized reasoning process; and **(ii)** a fuzzy system identification algorithm. The reasoning mechanism addresses the following: **(a)** the implementation of the information in each rule; **(b)** the aggregation of information among a set of rules; and **(c)** fuzzy logic inferred values mapping into crisp equivalent values. The system identification process can be divided into two parts: structure identification and parameter identification. The structure identification problem consists of the fuzzy rules generation and the construction of the input-output membership functions. In the parameter identification process, two steps are performed. In the first step, the system parameters (i.e., input-output membership functions parameters and the reasoning parameters) are optimized by minimizing a *performance index*. In the second step, the input-output membership parameters are tuned the same way as ordinary system identification methods.

P517312.PDF [Page: 44 of 77]

3.1 Fuzzy Structure Identification

Fuzzy structure identification is the process of assigning the optimum number of rules, significant input variables, input and output membership functions, and the degree of overlap between the membership functions required for the fuzzy model. These are briefly discussed in this section.

We first cluster the output space [4], and then derive the input space fuzzy partition by projecting the output space partition onto each input space, separately. The output fuzzy clustering is carried out using Fuzzy C-Means (FCM) algorithm [5]. The idea of fuzzy clustering is to divide the output data into fuzzy partitions that overlap each other. The membership grades are obtained through an iterative procedure as follows:

$$u_{ik,l} = \left[\sum_{j=1}^{c} \left(\frac{\sqrt{y_k - v_{i,l-1}}}{\sqrt{y_k - v_{j,l-1}}} \right)^{\frac{2}{m-1}} \right], \qquad (2)$$

where

$$v_{i,l} = \frac{\sum_{k=1}^{N} (u_{ik,l})^m y_k}{\sum_{k=1}^{N} (u_{ik,l})^m}. \qquad (3)$$

and N is the number of data, $u_{ik,l}$, $v_{i,l}$ are the membership grade of the output y_k in the cluster i and the center of the cluster i, respectively, at the l^{th} iteration. The following cluster validity index [6] is used for assigning the optimum number of output clusters, and hence, the number of rules, in the fuzzy model:

$$S_{CS} = \sum_{k=1}^{N} \sum_{i=1}^{c} (u_{ik})^m \left((y_k - v_i)^2 - (v_i - \overline{v})^2 \right), \qquad (4)$$

P517312.PDF [Page 45 of 77]

where $\bar{v}$ is the weighted mean of data considering their membership to each of the clusters defined as:

$$\bar{v} = \frac{1}{\sum_{i=1}^{c}\sum_{k=1}^{N}(u_{ik})^m} \sum_{k=1}^{N}\sum_{i=1}^{c}(u_{ik})^m y_k . \qquad (5)$$

The optimum number of clusters c corresponds to minimum s_{cs}. In most cases, c is equal to the number of rules n for the fuzzy model. The weighting exponent m controls the extent of membership sharing between output fuzzy clusters in the data set:

$$S_T = \sum_{k=1}^{N}\left(\sum_{i=1}^{c}(u_{ik})^m\right)(y_k - \bar{v}), \qquad (6)$$

An appropriate value for m is chosen to make S_T equal to a constant parameter $z/2$, where z is defined as [6]:

$$z = \sum_{k=1}^{N}\left[\left(y_k - \frac{1}{N}\sum_{j=1}^{N} y\right)^2\right]. \qquad (7)$$

The initial cluster centers for the FCM algorithms are assigned through hard clustering techniques [7].

3.2 Reasoning Mechanism

For the crisp input $x^* = (x_1^*, x_2^*, ..., x_r^*)$, the fuzzy output of the system is obtained according to Mamdani-type inference using the following formulation:

$$E(y) = \left(1 - S_p\left[T_p\left[\tau_1(x^*), \bar{D}_1(y)\right], ..., T_p\left[\tau_n(x^*), \bar{D}_n(y)\right]\right]\right) \qquad (8)$$

where τ_i, called the *"rule degree of firing"*, is computed as:

P517312.PDF [Page: 46 of 77]

$$\tau_i(x^*) = T_q\left(B_{i1}(x_1^*), B_{i2}(x_2^*), \ldots B_{ir}(x_r^*)\right), \tag{9}$$

and

$$\overline{D} = 1 - D_i(y).$$

where r is the number of antecedents, n is the number of consequent, and S_p is the *binary* t-conorm operator computed as [8]:

$$S_p(a_1, a_2) = \left(a^p + b^p - a^p b^p\right)^{1/p} \tag{10}$$

The operator $T_\chi(\chi = p,q)$ is the n-ary t-norm operator calculated as:

$$T_\chi(a_1, a_2) = 1 - S_\chi((1-a_1),(1-a_2)). \tag{11}$$

The optimum values of the inference parameters are identified through minimizing:

$$PI(p,q,\alpha) = \sum_{k=1}^{N} (y_k - \hat{y})^2 / N, \tag{12}$$

where y_k is the actual output and $\hat{y}_k$ is the model output. The input-output membership functions that have already been identified in the structure identification phase are approximated by trapezoidal functions, and then an incremental tuning procedure is used to adjust the membership function parameters based on the training data set and the performance index above. Finally, the crisp output is obtained using the *Basic Defuzzification Distribution* method as follows [9]:

$$y^* = \frac{\int_{y_0}^{y_1} y[E(y)]^\alpha dy}{\int_{y_0}^{y_1} [E(y)]^\alpha dy} \qquad 0 \le \alpha \le \infty. \tag{13}$$

3.3 Fuzzy Modeling of Cardiovascular Response

The fuzzy modeling approach presented above has been used for modeling the dynamic cardiovascular responses obtained from the tilt table experiments. Two groups of data for pitch and roll orientations were used as the training sets to generate the corresponding fuzzy model. In each group of data, the experimental observations from different subjects were combined together to form the corresponding training set. In a training set, the inputs are tilt rates and dwell times. The outputs are the corresponding blood pressure indices defined in Fig 9. The experiments on the tilt table were performed for a dwell time of 7, 15, and 30s. The tilt rate was chosen as 15, 30, and $45^{\circ}s^{-1}$. Different subjects' cardiovascular responses have been recorded for multiple combinations of the tilt rate and dwell time. Since, the tilt-table used for the experiments reported in [1] did not have an automatic control of dwell time duration, the dwell times in some experiments slightly differ among themselves.

Figure 10 presents a comparison between the developed fuzzy model and the actual training data extracted from experiments for every blood pressure index and pitch/roll orientation. Figure 11 shows six sets of fuzzy rules corresponding to the available two groups of data, i.e., 3 sets of rules for pitch rotation and 3 for roll rotation. Every rule base is a 2-input single output mapping. The inputs are tilt rate and dwell time. The output is one of the blood pressure indices defined in Figure 9. Table 2 summarizes the fuzzy modeling parameters (i.e., inference parameters in section 3.2), number of rules (n=*5, 6, or 7*) required for accurate inference, and levels of fuzziness m (as introduced in section 3.1) for each of the sets of rules shown in Figure 11. Figure 12 shows the pressure surfaces for the predefined physiological indices obtained for the tilt rate varying

P517312.PDF [Page: 48 of 77]

continuously from 15 to 45 deg/sec and the dwell time varying from 7 to 30 sec. Figure 13 shows a comparison of the effect of varying dwell time on the blood pressure indices for both pitch and roll rotations when the tilt rate is fixed at 45 deg/sec. The sets of curves in Figure 13 were obtained by slicing the surfaces in Figure 12 for each index separately.

3.4 Discussion

Different subjects can exhibit distinct cardiovascular response to orthostatic stress. The training sets used to build the fuzzy models embody the response of ten different subjects. Hence, the models developed in this work can be used to infer (with a certain accuracy) the blood pressure indices that describe the cardiovascular response for different tilt scenarios and for various subjects. This would be beneficial to *a priori* prediction of the tolerance of a pilot's cardiovascular response to a specific flight maneuver. Such maneuver can have similar or different HU-HD and HD-HU orientations and different tilt rates or dwell times. Hence, in addition to the dynamic models introduced in section 2 to predict BP changes on the instant-by-instant basis, the fuzzy models, which are not explicit for a specific tilt rate, dwell time, or subject, can be used for a *priori* prediction of cardiovascular response indices.

Moreover, the fuzzy models of the blood pressure indices can also be used to estimate the most favorable orientation for the recovery from hypogravity to hypergravity transitions during flight maneuvers. For instance, one simple form of a split-S maneuver is when a specific subject undergoes the transition from the normal gravity (or hypergravity) to hypogravity in pitch rotation and after a certain dwell time at the hypogravity transits to hypergravity in roll rotation. Another split-S maneuver can involve a transition from the

normal gravity (or hypergravity) to hypogravity in roll rotation, followed by the transition to hypergravity in pitch rotation. A more involved split-S maneuver would be a sequence of the aforementioned basic split-S maneuvers with varying pitch/roll rotations, dwell times, and tilt rates on every transition. Using the fuzzy models for blood pressure indices developed in Section 3, one can break down every maneuver into two transitions: (i) HU-to-HD (or the corresponding transition from the normal or hypergravity to hypogravity), and (ii) HD-to-HU (or the corresponding transition from the hypogravity to the hypergravity or normal gravity). For the first transition (whether it is performed in pitch or roll rotation), we can use the proper initial status (HD drop model) to determine the blood pressure change in such a transition given the corresponding tilt rate and dwell time. For the second transition, we can use the maximum drop in BP and final BP status models to determine the corresponding blood pressure change both during the HD-HU phase and after the subject recovers from the orthostatic stress. By simply predicating the pressure indices using the fuzzy models for every transition, one can monitor the cardiovascular response of a pilot throughout each maneuver. Therefore, any profound effect on the cardiovascular response, i.e., an intolerable drop of BP can be detected *a priori* and hence preventive measures can be developed and undertaken.

4. Conclusion

In this paper we have developed dynamic models for a typical subject's cardiovascular response in an attempt to predict the corresponding compensation during orthostatic stress. Two different approaches were used to model the cardiovascular responses: (i) second-order discrete-time models for continuous instant-by-instant prediction of blood

P517312.PDF [Page: 50 of 77]

pressure response throughout a specific maneuver, and **(ii)** fuzzy logic models that can predict the blood pressure indices in a single/multiple consecutive maneuvers or split-S maneuvers using a set of rules and a fuzzy inference mechanisms.

Through experimental analysis, we verified that values of the parameters of the second-order dynamic model are subject-dependent as well as tilt scenario dependent. Hence, such an approach can be used for moment-by-moment prediction only if the type of the maneuver and its corresponding tilt rate and dwell time are known *a priori* and the corresponding subject's model is available.

On the other hand, the fuzzy logic modeling approach can be used to infer (with a predefined degree of accuracy) the cardiovascular response for different tilt rotation and for various subjects.

Fig. 1: *The setup for tilt-table experiments*

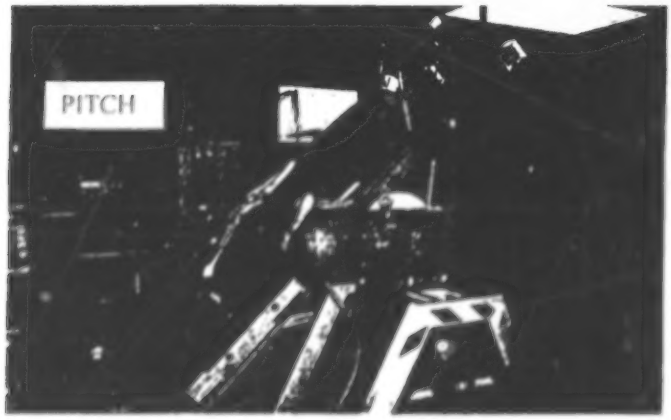

Fig. 2: *Pitch and Roll rotations*

P517312.PDF [Page: 53 of 77]

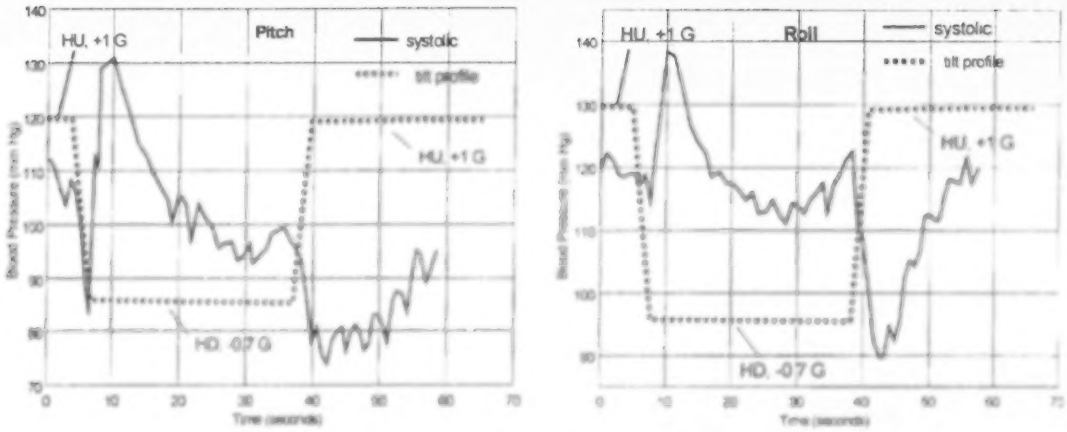

Fig. 3: *A typical response of the BP in mm Hg recorded at heart level during pitch rotation (left) and roll rotation (right) Dotted line shows the profile of G transition during a complete tilt motion*

P517312.PDF [Page: 54 of 77]

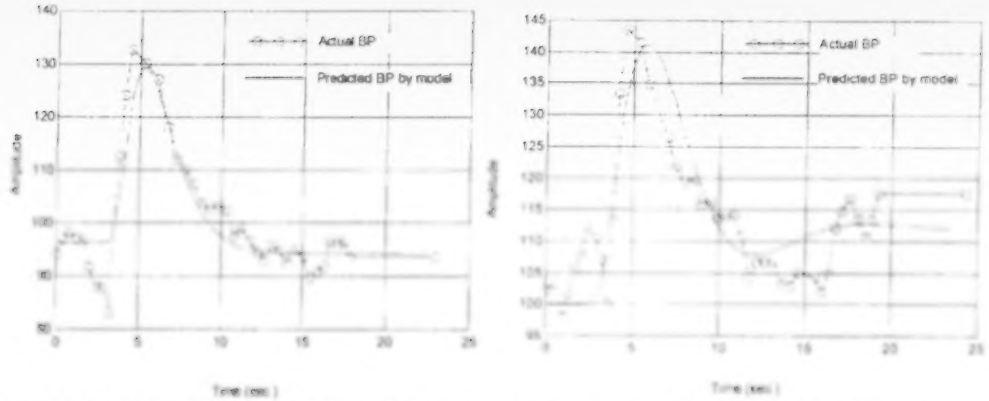

Figure 4: *Model for subject 1 from HU-to-HD in patch orientation (left) Model for subject 1 from HU-to-HD in roll orientation (right)*

P517312.PDF [Page: 55 of 77]

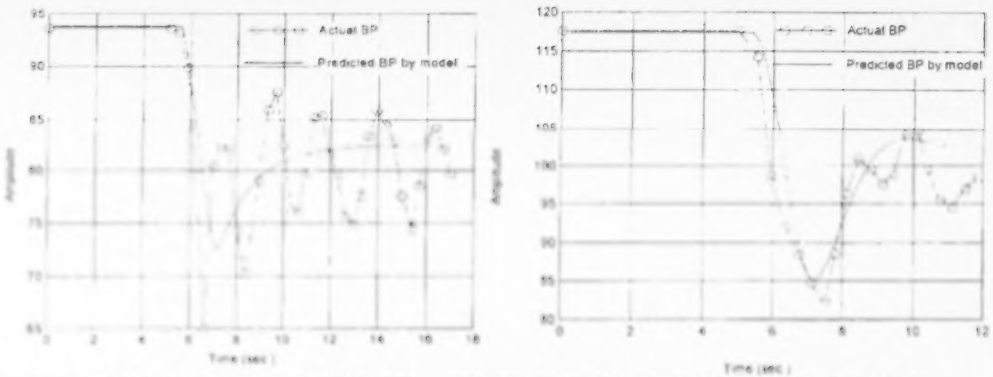

Figure 5: *Model for subject 1 from HD-to-HU in pitch orientation (left) Model for subject 1 from HD-to-HU in roll orientation (right)*

2517312.PDF [Page: 56 of 77]

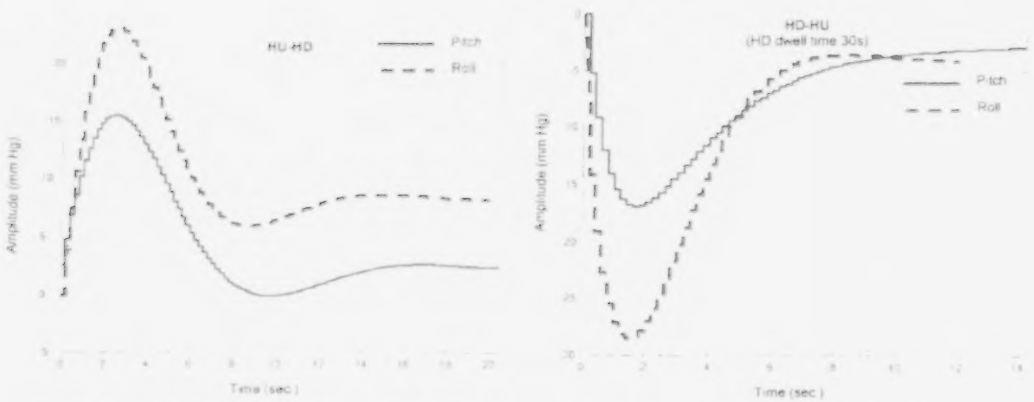

Figure 6: *BP changes predicted by the models during HU-to-HD transition in pitch and roll rotations (left) BP changes predicted by the models during HD-to-HU transition in pitch and roll rotations (right)*

8317312.PDF [Page: 57 of 77]

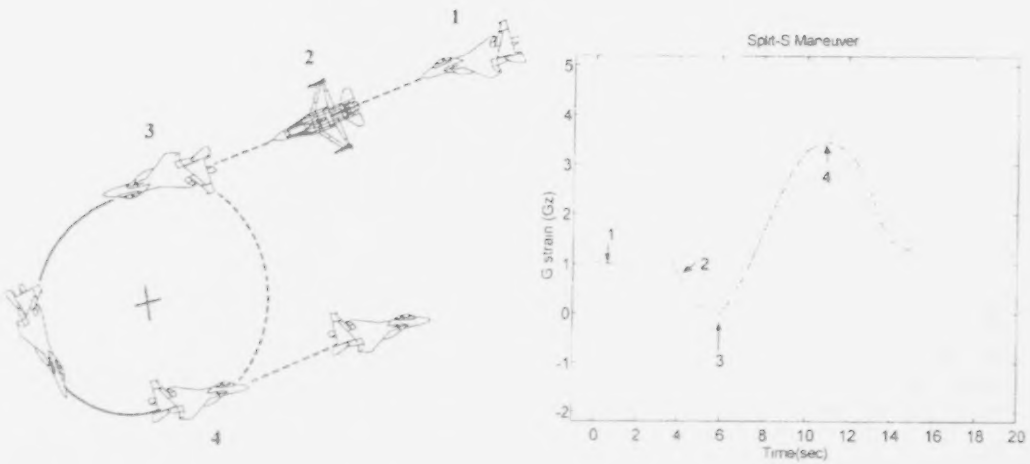

Figure 7: *An S-split maneuver and the corresponding G-force at every transition*

P917312.PDF [Page: 58 of 77]

IF U_1 *is* B_{11} *AND* U_r *is* B_{1r} *THEN* V_1 *is* D_{11} *AND*... V_s *is* D_{1s}
ALSO
.....
IF U_1 *is* B_{n1} *AND* U_r *is* B_{nr} *THEN* V_1 *is* D_{n1} ... *AND* V_s *is* D_{ns}

Figure 8: *The fuzzy input-output rules*

P517312.PDF [Page: 59 of 77]

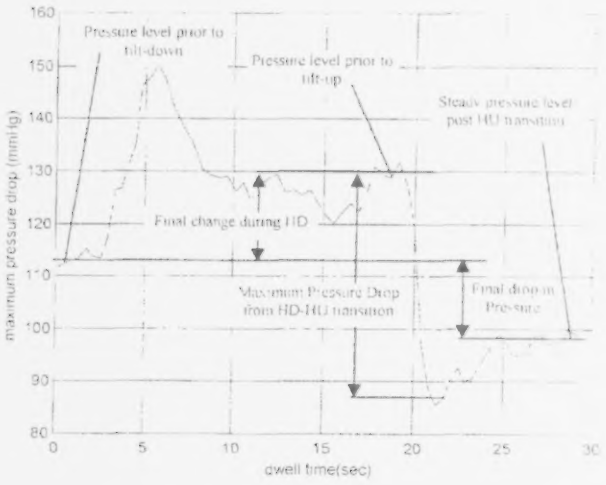

Figure 9: *Indices of a typical BP response to HU-HD and HD-HU transitions*

P517312.PDF [Page: 60 of 77]

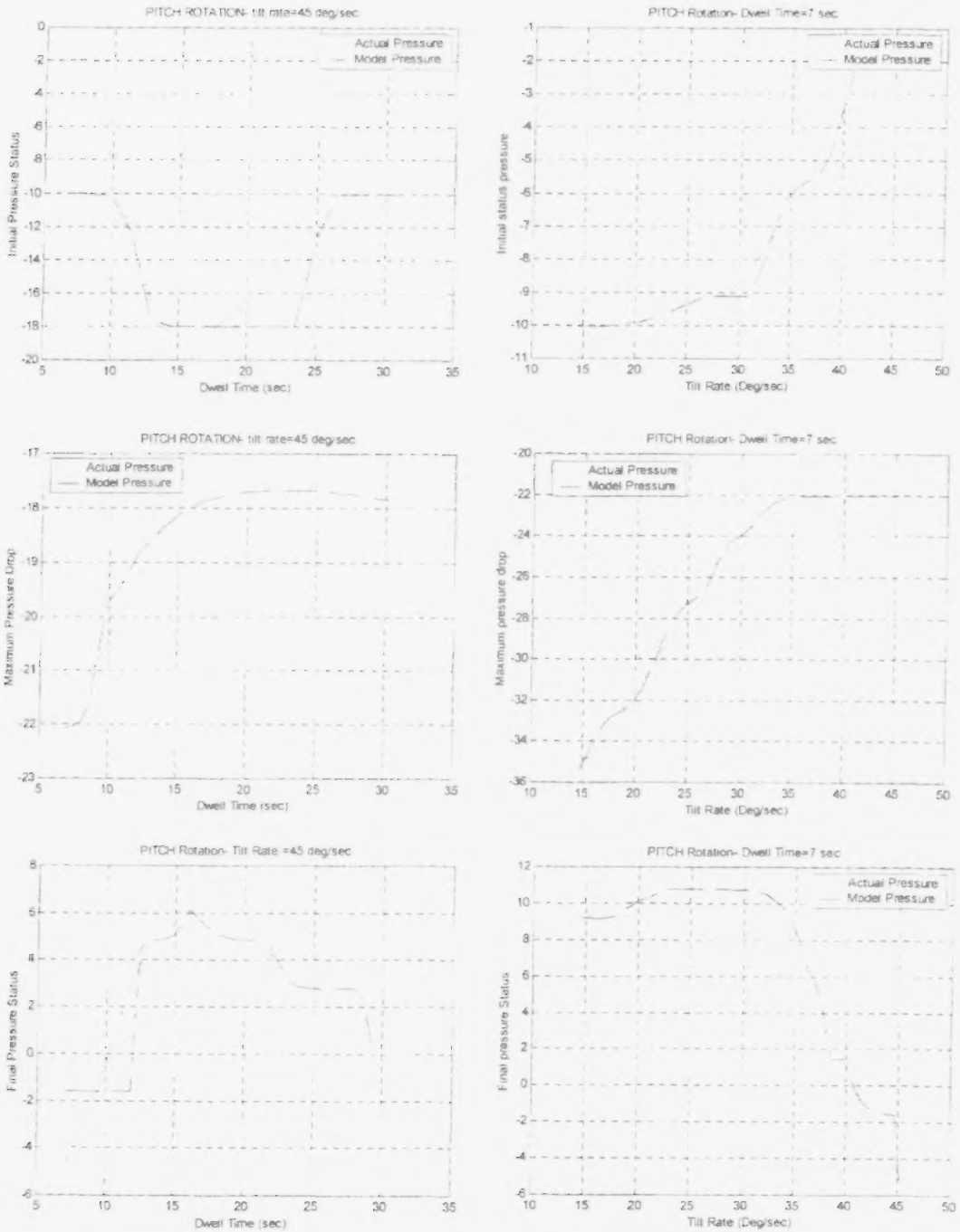

Figure 10: *comparison between the experimental data and the fuzzy models for pitch orientation*

P517312.PDF [Page: 61 of 77]

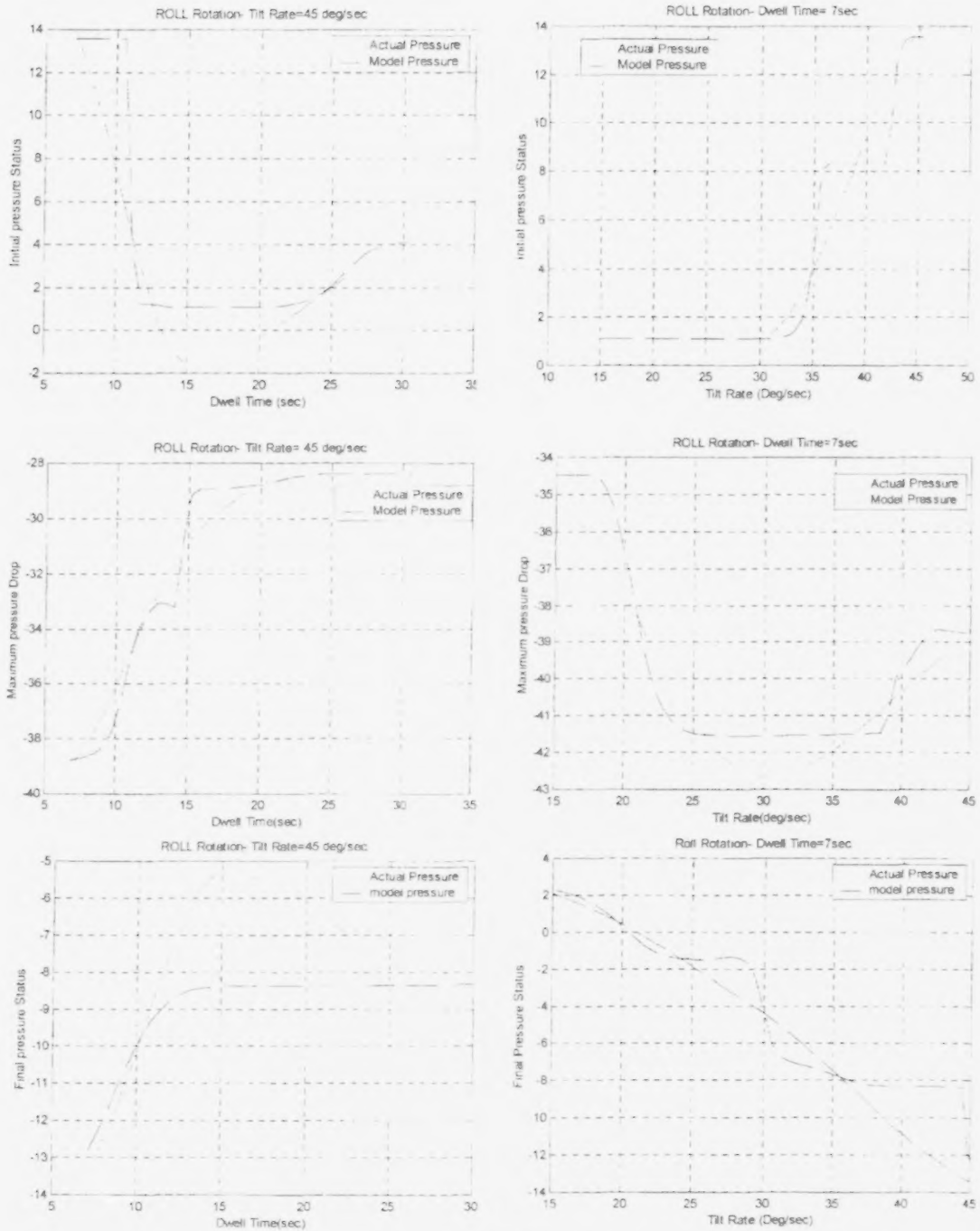

Figure 10 (cont'd): *comparison between the experimental data and the fuzzy models for roll orientation*

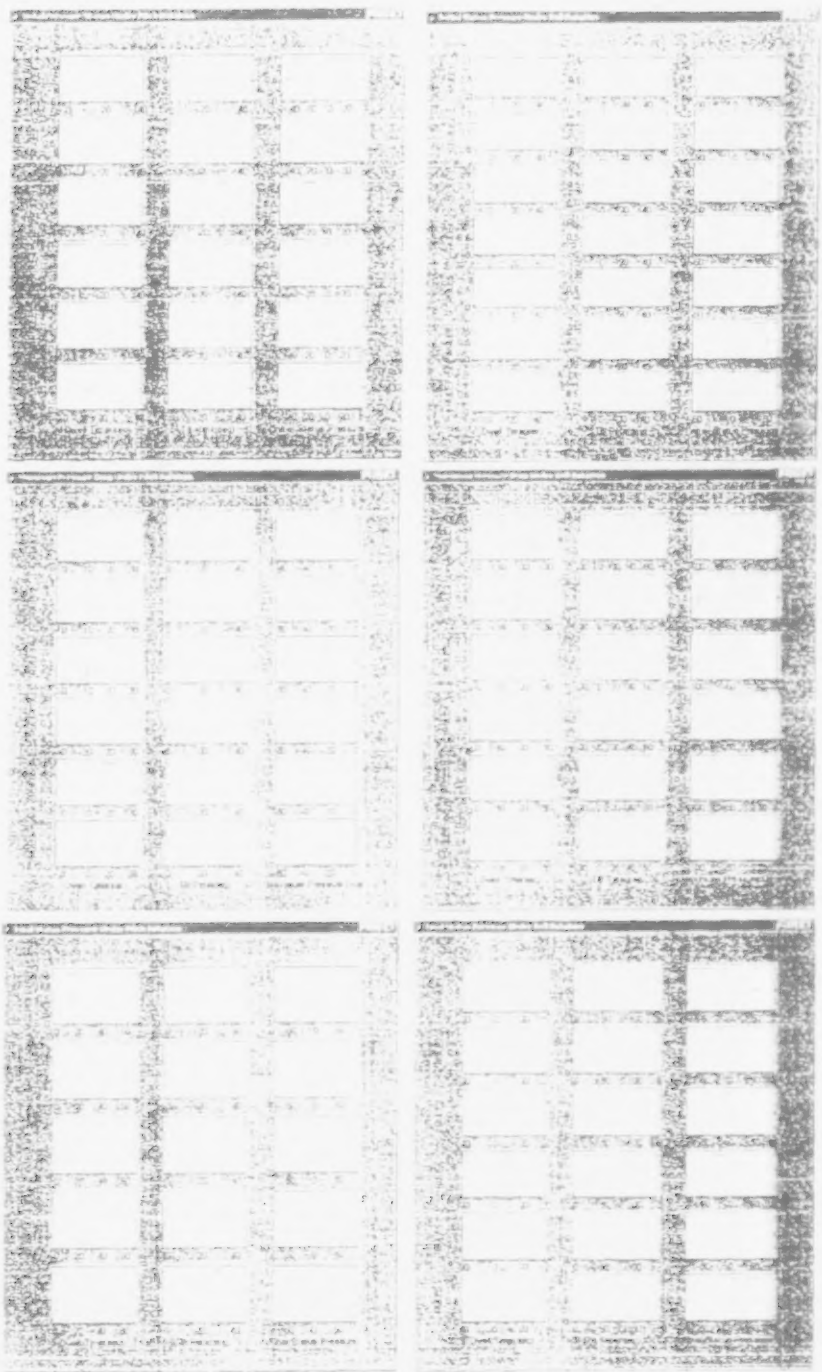

P517312.PDF [Page: 62 of 77]

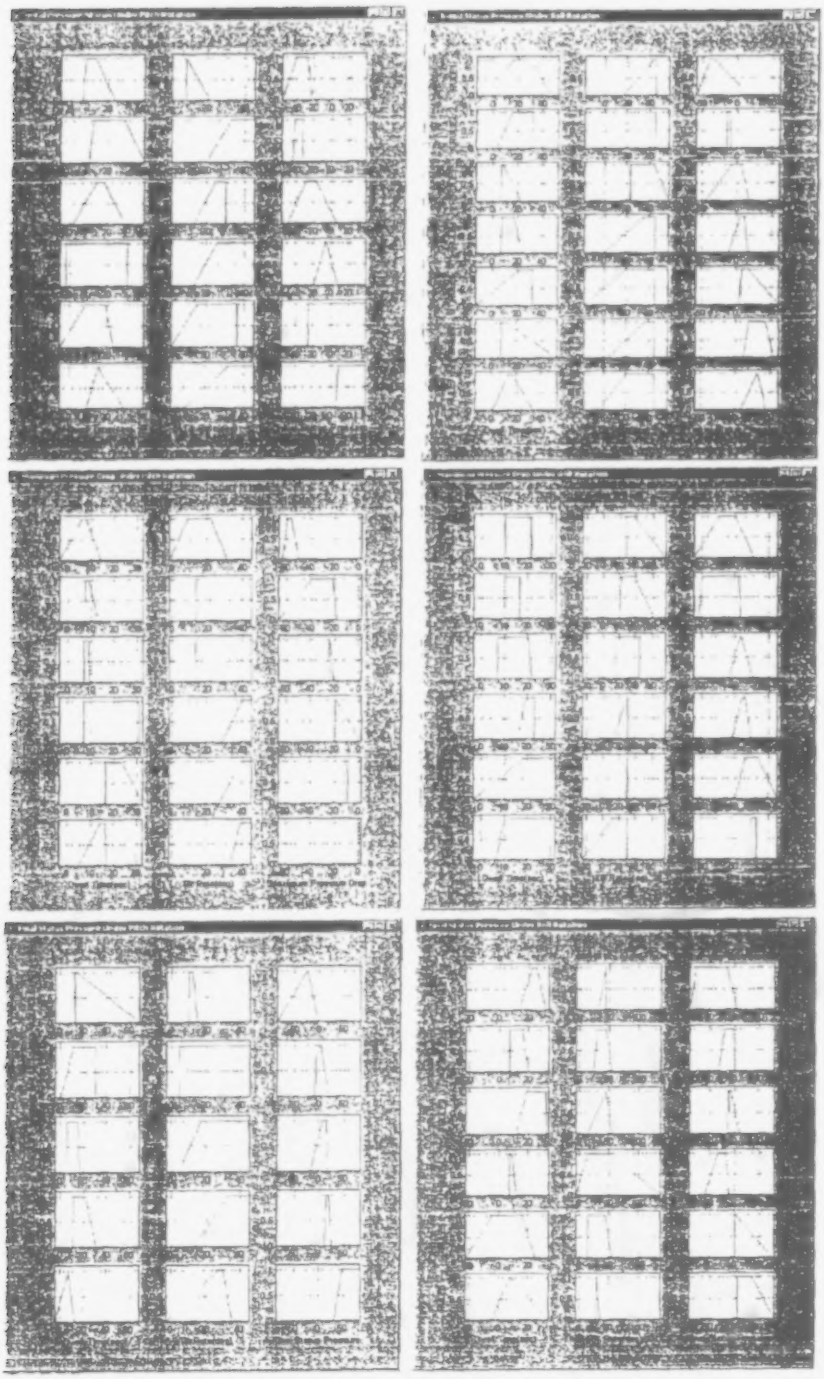

Figure 11: *The fuzzy models of the pressure indices for pitch/roll rotations*

P517312.PDF [Page: 63 of 77]

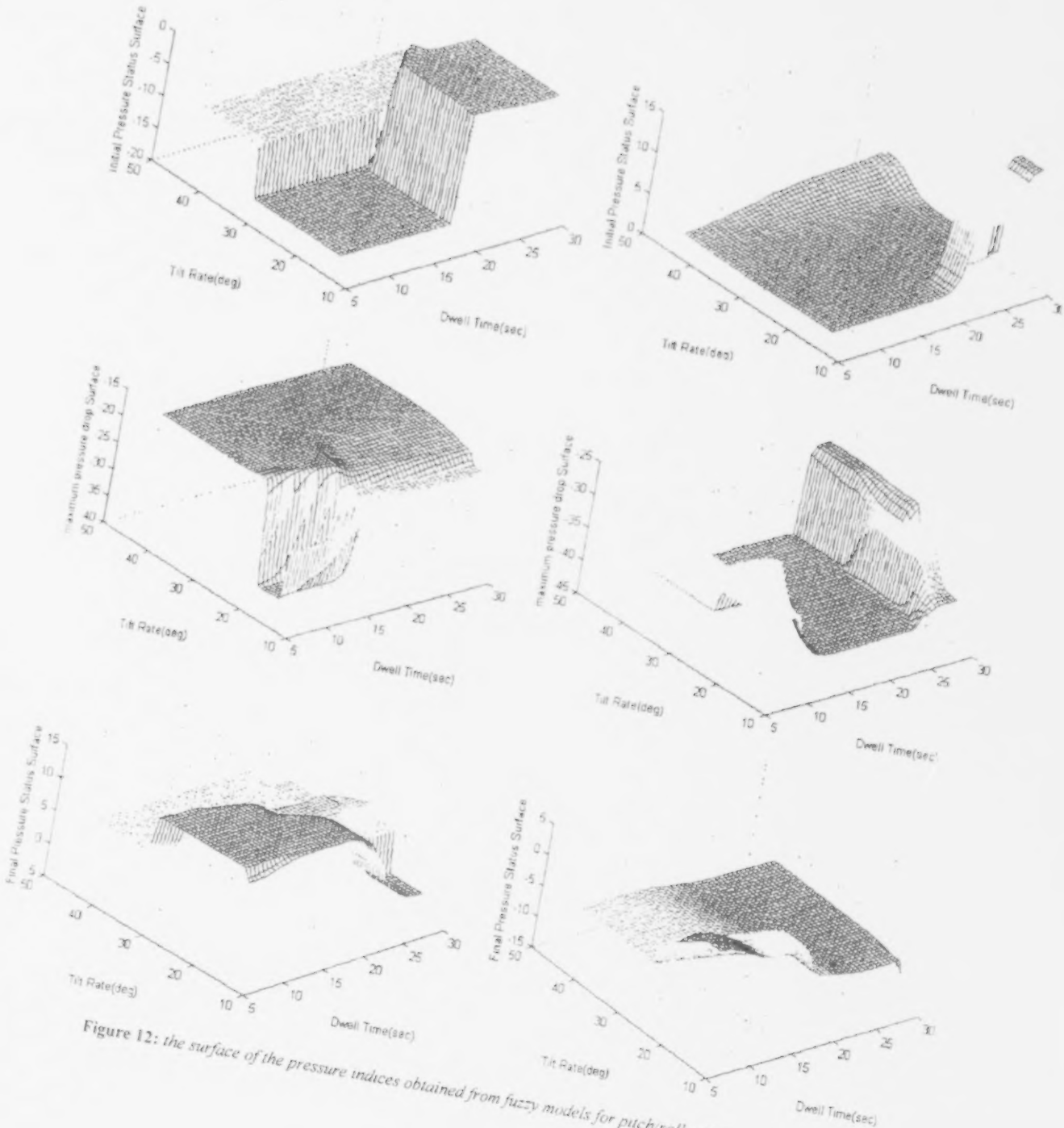

Figure 12: *the surface of the pressure indices obtained from fuzzy models for pitch/roll orientation*

P517312.PDF [Page: 64 of 77]

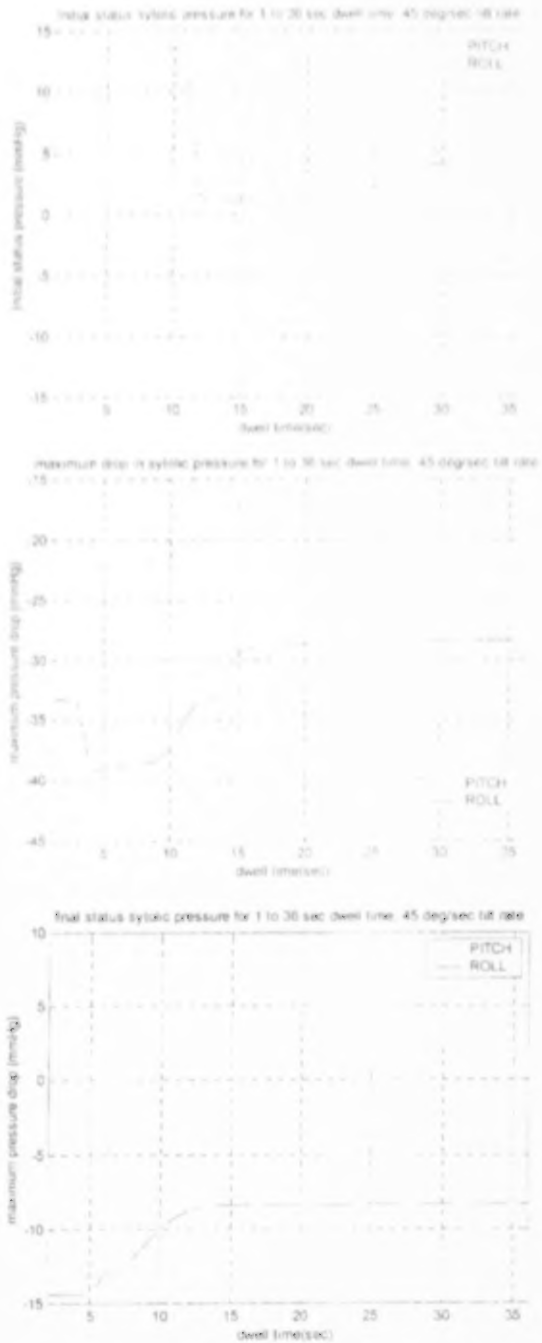

Figure 13: *The effect of varying the dwell time on the pressure indices for pitch/roll orientation*

Orient.	*Trans.*	*Model Parameters*	
		B-matrix	*F-matrix*
Pitch	HU-HD	-2.32 2.33	1.00 -1.89 0.90
Roll	HU-HD	-3.62 3.56	1.00 -1.90 0.91
Pitch	HD-HU	-4.40 4.35	1.00 -1.79 0.80
Roll	HD-HU	-7.88 7.81	1.00 -1.79 0.81

Table1: *Model parameters for subject 1 under pitch/ roll rotation (Refer to equation (1) for the definition of B and F matrices)*

Pressure index definition	Pitch Orientation		Roll Orientation	
	Inference parameters [p q α]	Rules & level of fuzziness [n m]	Inference parameters [p q α]	Rules & level of fuzziness [n m]
Drop In HD transition (Initial status)	[12 0 3 65]	[5 2.6]	[23 0 9 122]	[7 2.3]
Maximum pressure drop post HU transition	[22 1 6 115]	[6 2.5]	[45 5.5 34]	[6 2.5]
Final status pressure	[17 4 3 61]	[5 2.8]	[9 1.3 23]	[6 2.6]

Table2: *Fuzzy models' parameters*

Acknowledgment

This work has been supported by the research contract W7711-007683/A issued by the Canadian Department of National Defence, Defence and Civil Institute of Environmental Medicine.

PS17312.PDF [Page: 66 of 77]

References

[1] Cheung B., Hofer K., and Goodman L.; "The effect of roll vs. pitch rotation in humans under orthostatic stress"; Aviation, Space, and Environmental Medicine; Vol. 70, No. 10, pp.966-974; 1999.

[2] Von Beckh HJ. ; "Human reactions during flight to acceleration preceded by or followed by weightlessness; Aerospace Medicine; Vol. 30; No. 9; pp. 391-409; 1959.

[3] Ljung L.; "System Identification-Theory for the User", Prentice-Hall, Eng.Cliffs, N.J, 1987.

[4] Sugeno M., Yasukawa T.; "A fuzzy-logic-based approach to qualitative modeling"; IEEE Transactions on Fuzzy Systems; Vol.1; No.1; 1993.

[5] Bezdek J. C.; "Pattern Recognition with Fuzzy Objective Function Algorithms"; Plenum Press; NY; 1981.

[6] Emami M. R., Turksen I. B., Goldenberg A. A.; "A unified parameterized formulation for reasoning process in fuzzy modeling and control"; Fuzzy Sets and Systems; 2000.

[7] Ward J. H.; "Hierarchical grouping to optimize an objective function"; Journal of American Statistics Association; No. 58; pp.236-244; 1963.

[8] Schweizer B., Sklar A.; "Probabilistic Metric Spaces"; North-Holland; Amsterdam; 1983

[9] Yager R. R., Filev D. P.; "Essentials of Fuzzy Modeling and Control"; John Wiley & Sons; 1994.

[10] Von Beckh HJ; "Experiments with animals and human subjects under sub and zero-gravity conditions during the dive and parabolic flight"; Journal of Aviation Medicine; Vol. 25; pp.235; 1954.

[11] Prior ARJ, Adcock TR., McCarthy GW; "In-flight arterial blood pressure changes during –Gz to +Gz maneuvering; Aviation, Space, and Environmental Medicine; Vol.64; pp.428; 1993.

[12] Lehr AK, Prior ARJ, Langewouters G, et al.; "Previous exposure to negative Gz reduces relaxed +Gz tolerance"; Aviation, Space, and Environmental Medicine; Vol.63; pp.405; 1992.

[13] Diedrichs RW; "Adverse effect of negative Gz on subsequent high positive Gz: a need for research and education"; Aeromedical and Training Digest; Vol. 4, No. 36; pp.8; 1990.

[14] Michaud VJ, Lyons TJ, Hansen CM; "Frequency of the push-pull effect in USAF fighter operations"; Aviation, Space, and Environmental Medicine; Vol.68; pp.201; 1998.

PS17512.PDF [Page: 67 of 77]

Fig. 1: The setup for tilt-table experiments

Fig. 2: Pitch and Roll rotations

Fig. 3: A typical response of the BP in mm Hg recorded at heart level during pitch rotation (left) and roll rotation (right). Dotted line shows the profile of G transition during a complete tilt motion

Fig. 4: Model for subject 1 from HU-to-HD in pitch orientation (left). Model for subject 1 from HU-to-HD in roll orientation (right).

Fig. 5: Model for subject 1 from HD-to-HU in pitch orientation (left). Model for subject 1 from HD-to-HU in roll orientation (right).

Fig.6: BP changes predicted by the models during HU-to-HD transition in pitch and roll rotations (left). BP changes predicted by the models during HD-to-HU transition in pitch and roll rotations (right)

Figure 7: An S-split maneuver and the corresponding G-force at every transition

Figure 8: The fuzzy input-output rules

Figure 9: Indices of a typical BP response to HU-HD and HD-HU transitions

Figure 10: comparison between the experimental data and the fuzzy models for pitch orientation

Figure 11: The fuzzy models of the pressure indices for pitch/roll rotations

Figure 12: the surface of the pressure indices obtained from fuzzy models for pitch/roll orientation

Figure 13: The effect of varying the dwell time on the pressure indices for pitch/roll orientation

P517312.PDF [Page: 68 of 77]

Dependency of Cardiovascular Responses on Head Orientation in Hypogravity and Hypergravity Transitions

ZIREN LU**, BOB CHEUNG*, ALEX KAPPS**, AARON GALLUZZI**, WILLIAM MELEK**, KEVIN HOFER*

** Defence and Civil Institute of Environmental Medicine (DCIEM), 1133 Sheppard Avenue West, Toronto,Ontario, Canada, M3M 3B9;*

*** Engineering Services Inc. (ESI), 1 Bedford Road, Unit #5, Toronto, Ontario, Canada, M5R 2J7*

Background It has been known since 1953 that pre-exposure to less than +1 G_z will reduce subsequent +G_z-tolerance. With few exceptions, during operational flying, the transition from hypogravity to hypergravity involves roll as well as pitch rotations. Generally, there exist four possible combinations of these rotations during ±G_z transition (i) pitch during both transitions from +1 G_z to hypogravity and from hypogravity to +1 G_z, (ii) roll during both transitions from +1 G_z to hypogravity and from hypogravity to +1 G_z, (iii) pitch during transition from +1 G_z to hypogravity followed with roll during transition from hypogravity to +1 G_z; and (iv) (iii) roll during transition from +1 G_z to hypogravity followed with pitch during transition from hypogravity to +1 G_z. As a follow-up to our previous study (8), we analyzed separately the effects of roll vs pitch rotation while undergoing transition from +1 G_z to hypogravity (head-down, HD) and transition from hypogravity to +1 G_z (head-up, HU) on a tilt table. We also examined the effects of different head-down dwell time and offset (i.e., rotation) rate in both pitch and roll rotations. **Methods** Eleven subjects were rotated at 15°s^{-1}, 30°s^{-1} and 45°s^{-1} from head-up (HU) at 15° relative to gravitational vertical to 135° head-down (HD) and back to the HU position after different HD dwell times. HD dwell times were set at 7, 15, and 30s. The subjects were rotated about the interaural axis (pitch) and about the naso-occipital axis (roll). Both the HD dwell times and axes of rotation were randomized within and across subjects. Systolic and diastolic blood pressure (BP) were recorded during HD-HU maneuver. **Results** Repeated measures analysis of variance has shown that the magnitude of the BP decrease induced by the HD maneuver is significantly higher ($p < 0.05$) in pitch than in roll while the decrease in BP induced by HU maneuver is significantly higher ($p < 0.05$) in roll than in pitch for all HD dwell time at offset 45 °s^{-1}. The orientation and rotation rate have also significant effect on BP drop in HU to HD ($p < 0.002$, $p < 0.005$) and HD to HU ($p < 0.003$, $p < 0.02$) maneuvers. **Conclusions** Our results suggest that among the four rotation combinations, roll rotation to HD and pitch rotation back to HU will induce least decrease in BP. The maximum decrease in BP occurs with pitch rotation to HD and roll rotation to HU. The working hypothesis analyzed in this paper is that the results can be explained on the basis of well-known otolith-cardiovascular reflex and bi-directional sensitivity of vestibular otolith organs that contribute to BP compensation during pitch, but not during roll. Follow-up elaborate experiments are being designed to further examine our results and the working hypothesis. **Keywords** orthostatic hypotension, vestibular, G-tolerance, otolith receptor, otolith-cardiovascular reflex

I. INTRODUCTION

More than fifty years ago evidence has appeared that alternating weightlessness and hypergravity may result in decreased in-flight G-tolerance and lowered efficiency of physiological recovery (4,5). In-flight study (22), a centrifuge investigation (17), and an anecdotal report (10) also indicated that there is a definite deleterious effect on +G_z tolerance when the pilot is subjected to the transition of negative to positive G_z. This evidence is further collaborated by a recent comprehensive in-flight study (33).

Maneuvers of G-transition ranging from 0 to +0.5 G_z for 3.5 to 5 seconds are common in air combat training missions (19). One common method used in a fighter aircraft to acquire tactical advantage over the opponent is the Split-S maneuver (see Fig 1), which involves "unloading" the aircraft prior to accelerating. With few exceptions, this maneuver involves rolling and pulling all the G aerodynamically available. As the following example shows, a certain percentage of these and similar maneuvers might result in decreased in-flight G-tolerance and subsequent accidents. In 1995, two Canadian CF18 fighter jets conducted 1 v 1 air combat training. Following a standard butterfly split, the two aircraft turned head-on and established a left-to-left pass with the #2 aircraft approaching from above. The mishap pilot initiated a 6.4 Gz "Split-S" turn from above the Lead aircraft. Prior to completing this turn and with the aircraft nose 40 degrees below the horizon, radial acceleration (Gz) was relaxed and the aircraft rolled to an inverted, nose low, attitude. The aircraft gathered speed as the dive angle steepened, and impacted the ground in a near vertical attitude at approximately 700 KCAS, or Mach 1.12. The pilot did not eject. The flight profile was consistent with Gz-induced loss of consciousness (G-LOC) and the investigation focused on the pre-crash physiological environment experienced by the mishap pilot. Data recorded by the Cold Lake Air Combat Maneuvering Range (ACMR) revealed that the pilot experienced approximately 8 seconds of relative negative Gz immediately prior to commencing the "Split-S" maneuver. It is estimated that the alternating hypo and hypergravity

P517312.PDF [Page: 69 of 77]

present in this accident has reduced the pilot's Gz tolerance by approximately 2.9 Gz.

Our previous study (8) was designed to investigate arterial pressure changes under orthostatic stress in either pitch or roll rotations by exposing subjects to head-up (HU, 1G) to head-down (HD, <1G) and back to HU (1G) transitions using a tilt table. The tilt table used is shown in Fig. 2. Fig. 3 shows typical pitch and roll rotations considered in this paper. The results of the current paper concur with the statistical analysis results presented in (8) and indicate that the human cardiovascular system might have different responses to orthostatic stress induced by the pitch and roll rotations.

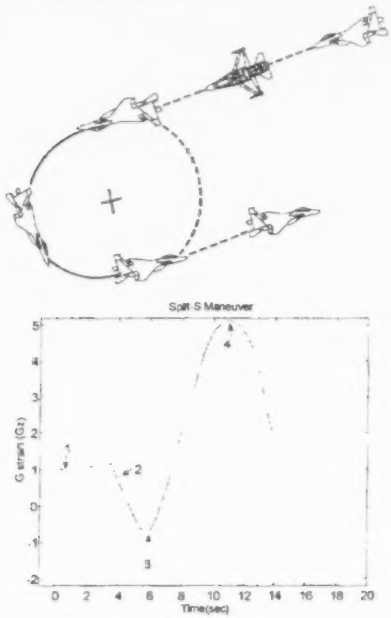

Fig. 1: *An S-split maneuver and the corresponding G-force at every transition*

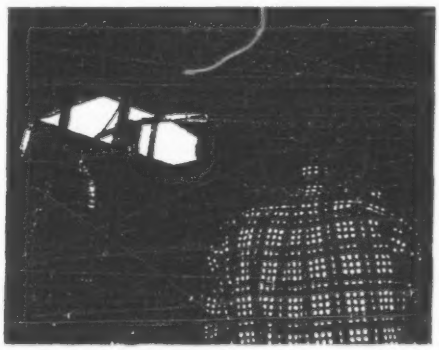

Fig. 2: *The setup for tilt-table experiments*

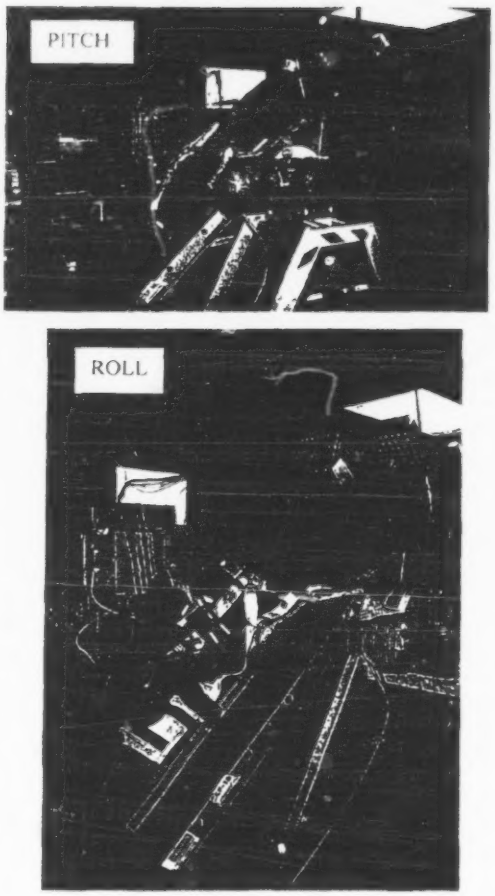

Fig. 3: *Pitch and Roll rotations*

The effects of the point roll or unloaded barrel roll maneuver on the subsequent increase in acceleration deserve the special attention in the context of pilots' protection due to the experimentally verified lower efficiency of blood pressure compensation associated with roll rotations than with pitch rotations. Vestibular receptors respond to gravitational forces and postural changes. These vestibular inputs constantly provide the central nervous system with information needed to produce corrections during on-going movements. The fact that blood pressure (BP) and oxygenation remain reasonably stable during rapid changes in posture suggests that corrections start at the beginning of a movement that is likely to affect homeostasis. For example, recent studies in decelerate rats (29) demonstrated that changes in sympathetic outflow were elicited by pitch rotation (about the interaural axis) but

P517312.PDF [Page: 70 of 77]

not by roll rotation (about the naso-occipital axis). In humans, clinical observations (19) indicated that a significant number of patients with peripheral vestibular disease were susceptible to orthostatic hypotension after standing from a supine position. In (8), we have formulated a hypothesis that there exists a vestibulo-cardiovascular reflex that can affect circulation and blood pressure regulation under orthostatic stress. Along the same lines, we recently investigated the otolith-cardiovascular reflex that had been first formulated in conjunction with animal studies (29) and recently confirmed in humans (31), (32), (33) (see the *Discussion* section for more detail).

In addition, the vestibular after-sensation of rolling is another factor that should not be ignored. Typically, in a roll of 2 rad·s^{-1} (or 100°, the sensation of roll dies away in 10 to 15 s (6). Recent surveys of civilian aerobatics pilots revealed that 12.7% reported persistent vertigo after aerobatics flight associated with -G_z exposure (27).

It is understood that ground-based devices are not capable of duplicating the precise maneuvers that could be performed by aircraft. This study was designed to investigate the primary effects of roll vs. pitch on cardiovascular response under orthostatic stress, by exposing subjects to head-up (HU) to head-down (HD) and back to HU maneuvers using a tilt table. This study is a follow-up to our earlier study on pitch vs. roll rotation (8).

II. METHODS

A. Subjects

Eleven healthy volunteers participated in this study. They had no known history of cardiovascular, ophthalmologic, oculomotor, or vestibular disorders. All subjects obtained medical approval from a physician to participate. The study was approved by the Defence and Civil Institute of Environmental Medicine (DCIEM) Human Ethics Committee. Informed consent was obtained from each of the subjects. Prior to the experiment, subjects were instructed to abstain from alcohol, over-the-counter and prescribed medications for at least 24 hours. All the subjects were familiarized with the experimental procedure and apparatus on separate days by exposing them to the roll and pitch rotation before data collection. Further, all of the subjects had pervious experience with the tilt table.

B. Apparatus

The motion stimulus is a man-rated electronic tilt table that can accommodate either a seated or standing subject with a range of 15° (HU) to 135° (HD) tilt. Zero degrees is considered to be the gravitational vertical. The angular velocity of the tilt table can be set from 5°s^{-1} to a maximum of 45°s^{-1} in 5° increments. The start angle, stop angle, and speed of rotation are pre-set prior to each run. A transducer attached to the tilt table registers the tilt angle, which was time-stamped for correlation with recorded physiological parameters. Axis of rotation for pitch and roll passed approximately through the mid body axis (at the umbilicus level) of the subject.

C. Procedure

A repeated measures, factorial design was employed with three factors: 1) orientation (pitch and roll); 2) HD dwell time (7, 15, and 30s); and 3) angular velocity of the tilt table, referred to as the *offset* rate (15°, 30°, and 45°). Each subject participated in experimental sessions, that were held at least one day apart, one for each of the HD dwell times and each of the offset rates where data could be gathered. Within each session, the subject was exposed to the two trials of different orientation; the order of the two orientations was also randomized. Each trial within each session was separated with a rest period of at least 10 min or until the subjects' BP stabilized and returned to their initial baseline. In the pitch orientation, the subject faced forward with their back against the tilt table and in the roll orientation, the subject faced sideways with the shoulder against the tilt table.

During each trial, the subject was positioned onto the tilt table with a loose harness and his feet secured to the stand plate. The subjects were instructed to close their eyes, relax, remain passive, and not to tense their muscles, especially during the rotation phase. Baseline measurements of arterial blood pressure (BP) and electrocardiogram (ECG) were recorded for at least 2 min at 15° relative to gravitational vertical. The subject was tilted to 135° head-down (HD) and remained in the HD position according to the assigned dwell time for that particular trial. The subject was then returned to the head-up (HU) position. The upright posture is one in which the utricular maculae are nearly horizontal. The direction of body tilt specifies the direction of the linear-acceleration vector acting on the statoconical membrane, and the sine of the angle of tilt specifies the magnitude of the shear force. Therefore, at 135° HD tilt, the magnitude of the linear acceleration vector acting on the statoconical membrane of the utricle is sin (135°) or -0.7071 G. BP and ECG were monitored throughout the HU-HD-HU maneuver, and after the tilt, until the BP returned to the baseline level.

A fingertip BP monitor (Finapres, Ohmeda In., Englewood, CO) was used for continuous measurement of systolic and diastolic BP with direct analog output to a Gould RS3600 polygraph (Valley View, OH). The servo self adjust function was disabled to ensure that the Finapres did not reset during critical measurement. The monitoring cuff was placed on the subject's middle finger of the left hand and secured on the third intercostal space at the sternal-costal junction with a modified work glove. ECG was continuously monitored using a Tectronics 408 electrocardiograph (Beverton, OR), sampling at 100 Hz. Three bipolar limb leads of VR (right arm), VL (left arm), and VF (left foot) were employed in this procedure.

P517312.PDF [Page: 71 of 77]

D. *Data Analysis*

For each tilt maneuver, we determined based on the systolic heart-level BP data the following indices: (i) the change in BP during HU to HD transition; and (ii) the change in BP during HD to HU transition. We designated the average of 6 BP measurement points immediately before the start of tilt down as the 'level before HD,' and the average of 6 BP measurement points after the completion of tilt up as the 'level after HU.' We designated the measurement of BP immediately before tilt up as the 'level before HU'. We also designated the change in BP from the 'level before HD' to 'level before HU' as the 'Drop in HD', and the change from the 'level before HU' to 'level after HU' as 'Drop in HU'. Analysis of variance on the repeated measures (longitudinal) data of BP was performed using the S-Plus/R statistical package (Insightful Inc.). We examined the effects of three factors on the 'Drop in HD' and 'Drop in HU': (i) rotation (pitch vs. roll); (ii) HD dwell time (7, 15, 30s); and (iii) offset rate (15, 30, 45°s^{-1}) Analysis of variance was followed by Contrast Analysis using paired t-test.

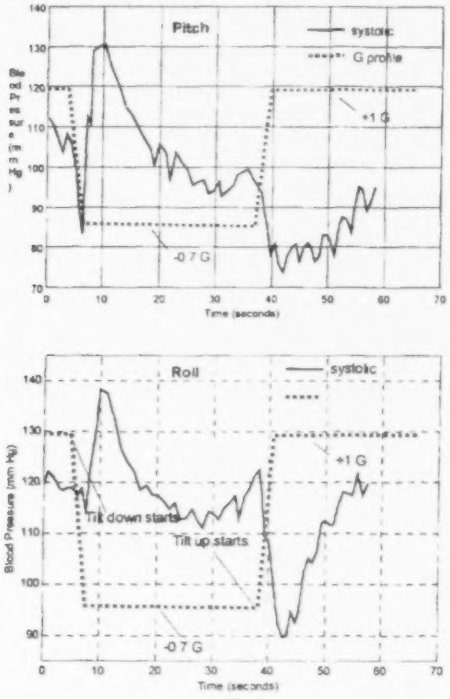

Fig. 4. *A typical response of the BP in mm Hg recorded at heart level during pitch rotation (top) and roll rotation (bottom) Dotted line shows the profile of G transition during a complete tilt motion*

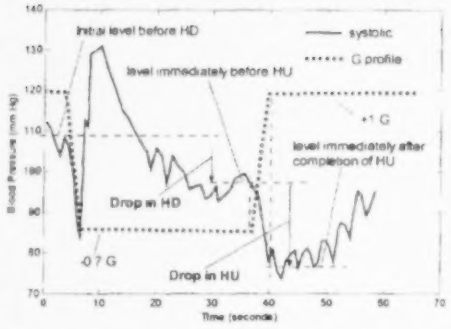

Fig. 5. *An average of 6 BP measurement points immediately before the start of tilt down and immediately after the completion of tilt up are defined as 'level before HD' and 'level after HU,' respectively The measurement immediately before tilt up is defined as 'level before HU'*

III. RESULTS

A typical response of BP from an individual male subject using 30s HD dwell time and onset/offset rate of45°s^{-1} is shown in Fig. 4. In all conditions, BP increases sharply to a maximum value following HU to HD tilt and then gradually decreases over the next 12~14s. After that time, BP either began to increase slightly or stayed relatively steady for the remainder of the HD period. Upon the initiation of HU tilt, BP immediately decreased and then recovered to a baseline in the next 5~18s.

A. *Pitch vs. Roll with different HD Dwell Time*

Repeated measures analysis of variance (ANOVA) of the data with different HD dwell time (onset rate fixed at 45°s^{-1}) indicates that the type of rotation (roll or pitch) and HD dwell times have a significant effect on the change (drop) in heart-level BP from the 'level before HD' to 'level before HU' ($p < 0.001$, $p < 0.001$). Similarly, the statistical analysis of the data with different HD dwell time (offset rate fixed at 45°s^{-1}) indicates that the type of rotation (roll or pitch) and HD dwell times have a significant effect on the drop in heart-level BP from the 'level before HU' to 'level after HU' ($p < 0.001$, $p < 0.02$) maneuvers. However, the interaction between HD dwell time and orientation was not significant. Fig. 6 (top) shows that the decrease in BP (defined in Fig. 5 as the Drop in HD and hence excluding the transitory increase in heart-level BP during the first few seconds following HD tilt) from BP value before the tilt to its HD steady-state value is less profound in roll rotation than in pitch rotation. One explanation of this fact is that the otolith sensors are not active during the roll rotation and hence the compensation in BP is only due to the baroreceptor-cardiovascular reflex, resulting on relatively low-

P517312.PDF [Page: 72 of 77]

efficiency compensation during the roll rotation than during the pitch rotation. At the same time it is shown in Fig. 6 (bottom) that Drop in HU (as defined in Fig. 5) is more significant for roll rotations than for tilt rotations for all the HD dwell times. This again can be explained by the fact that the otolith receptors are not invoked during roll rotations, and hence only one compensatory mechanism (baroreceptor-cardiovascular reflex) is present during roll rotations, whereas two compensatory mechanisms are present during pitch rotations (baroreceptor-cardiovascular reflex and otolith cardiovascular reflex). Note that since there is no difference between a subject's roll and pitch orientations while he/she is in head-down position on the tilt-table, the differences between pitch and roll diminishes in Fig 5 as the dwell time increases.

TABLE I. *Decrease in BP (HU to HD, OFFSET RATE = 45°s^{-1})*

	7s	15s	30s
Pitch	-1.22 ±3.98	-18.8 ±4.79	-8.8 ±3.79
Roll	+13.8 ±3.98	-1.5 ±4.79	-3.9 ±3.79

TABLE II. *Decrease in BP (HD to HU, OFFSET RATE = 45°s^{-1})*

	7s	15s	30s
Pitch	-21.7 ±4.11	-18.0 ±2.84	-18.0 ±3.24
Roll	-38.9 ±4.11	-30.8 ±2.84	-28.2 ±3.24

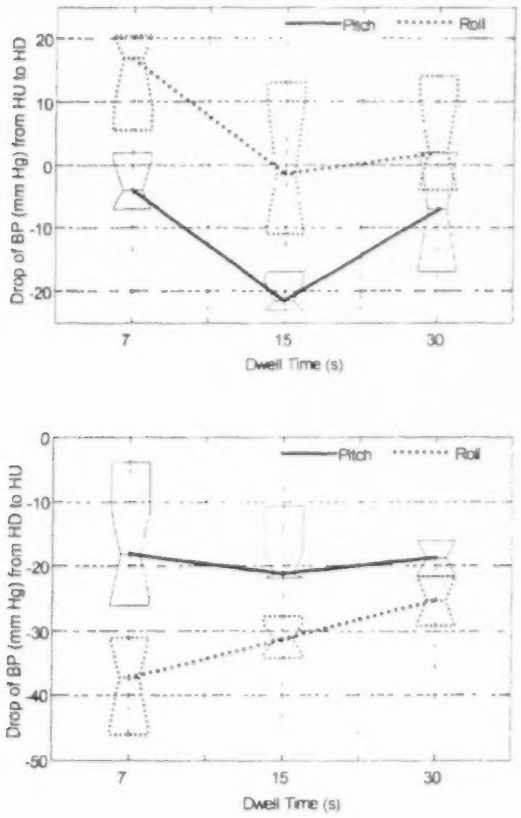

Fig. 6. *Decrease in Systolic BP as a function of HD dwell time and Type of Rotation (pitch or roll) during the HU-to-HD tilt transition (top) and HD-to-HU tilt transition (bottom) (error bars = SEM, Offset Rate is 45°s^{-1})*

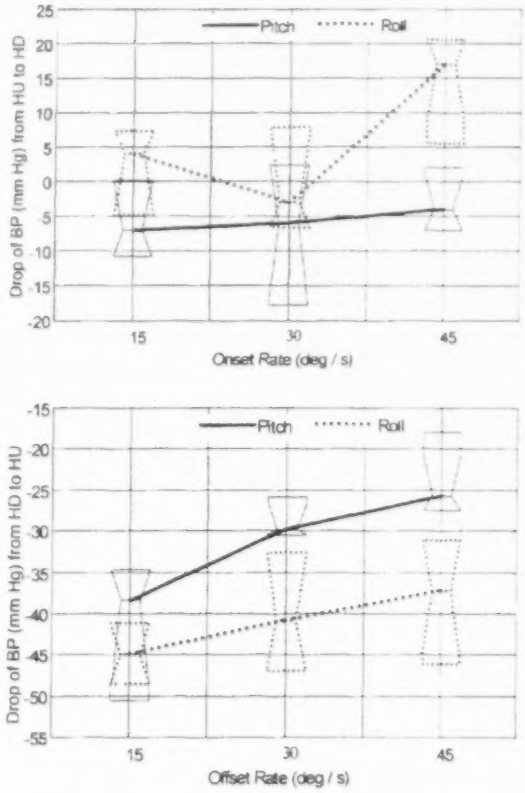

Fig. 7. *Decrease in systolic BP as a function of Onset /Offset Rate and Type of Rotation during HU-to-HD tilt transition (top) and HD-to-HU tilt transition (bottom) (error bars = SEM, HD dwell time is 7 seconds)*

P517312.PDF [Page: 73 of 77]

B. *Pitch vs. Roll with different Offset Rate*

The analysis results are depicted graphically in Figure 7. Repeated measures analysis of variance (ANOVA) of the data with different onset and offset rates (HD dwell time fixed at 7s) indicates that the type of rotation and onset rate had a significant effect on the change in BP (defined as Drop in HD in Fig. 5) following a tilt transition from HU to HD ($p < 0.002$, $p < 0.005$). At the same time, the change in BP (defined as Drop in HU in Fig. 5) following a tilt transition from HD to HU is also significantly affected by that the type of rotation (roll or pitch) and offset rate ($p < 0.003$, $p < 0.02$). However, the interaction between offset rate and orientation was also not significant.

Similar to the results reported in the previous subsection, it is seen from Fig. 7 (top) that the decrease in BP (defined in Fig. 5 as the Drop in HD) from BP value before the tilt to its HD steady-state value is less profound in roll rotation than in pitch rotation. At the same time it is shown in Fig. 7 (bottom) that Drop in HU (as defined in Fig. 5) is more significant for roll rotations than for tilt rotations for all onset and offset rates tested. We can further observe from Figure 7 (top) that for the case of pitch rotation, the Drop in BP index is independent of the onset rate. This can be possibly explained by the fact that otolith sensors, being the velocity sensors (35) effectively sense the rate of rotation and invoke an efficient compensation of BP.

IV. DISCUSSION

We are more accustomed to pitching than rolling movements. It is natural that a human's sensorial system naturally evolved to produce the maximally efficient compensation in BP responses when a human performs to pitching rather than rolling movements. Our results show that in HU to HD maneuvers the drop in BP at heart level is appreciably greater during pitch rotation than roll rotation. That is, the pitch orientation is more advantageous than the roll orientation in producing a faster and more effective cardiovascular compensation required to decrease heart-level BP and thereby minimize an excessive amount of increase in head-level BP caused by the transition from HU to HD position.

As far as a pilot who undergoes changes of G force from hypergravity to hypogravity and back to hypergravity is concerned, the highly efficient compensation associated with pitch rotations might yield undesirable physiological effects on the transition from hypergravity to hypogravity. It can be seen from Figs 6 (top) and 7 (top) that a pitch rotation from hypergravity to hypogravity causes a fast (as fast as 4-6 sec) and efficient decrease in heart-level BP and heartbeat rate that are naturally invoked by the human body to compensate for the increase in head-level BP due to the hypogravity acting in the Gz direction. This, in turn, immediately generates very disadvantageous initial conditions (low heart-level blood pressure and low heartbeat rate) for the upcoming hypo to hypergravity transition. Furthermore, our results (see Figs 6 (bottom) and 7 (bottom)) indicate that due to the more efficient cardiovascular compensation, the drop in BP during HD to HU tilt is smaller for pitch rotation than for roll rotation. Along with the aforementioned argument, this indicates that the human's sensorial and physiological systems are more effective in reducing the amount of decrease in BP at head level during the transition from HD to HU when the transition is performed in pitch configuration rather than in roll configuration.

A working hypothesis explaining the dynamic responses observed in our experiments can formulated on the basis of (i) well-known otolith-cardiovascular reflex, which has been first observed and investigated in mammals (29) and later in humans (31), (32); and (ii) bi-directional sensitivity of vestibular otolith organs that contribute to BP compensation during pitch, but not during roll (33). The existense of otolith-cardiovascular reflex means that blood pressure compensation during HD-HU and HU-HD transitions may be effectively invoked by at least two sensors: neck baroreceptors and otolith organs. Otolith organs are the sensors of the mammalian system that generate inputs signaling changes in linear motion of the head in space and produces cardiovascular responses to adjust and maintain stability of BP during changes in posture (31). It is also indicated in (8) that pitch and roll involve different stimulation of otolithic receptors: utricle and saccule. This may contributes to the difference in the responses of BP to different direction of acceleration (31).

Implication of Current Findings

In aerobatic maneuvers the pilot may experience changes of G force: from hypergravity to hypogravity and back to hypergravity, similar to that in our study induced by using a tilt-table. Such a maneuver can be divided into two periods: (*Period 1*) beginning of hyper-to-hypogravity transition until the beginning of hypo-to-hypergravity transition, (*Period 2*) remainder of the maneuver starting from the end of Period 1. The overall drop in BP during the entire maneuver of this sort will be the summation of drops during the first and second periods (see Fig 5 for more insight). Our results presented in Figs 6 and 7 indicate that during the first period, a pitch rotation will induce larger drop in BP than roll rotation. During the second period, a roll rotation will induce larger drop in BP than pitch rotation. Therefore, it is reasonable to postulate that the overall drop in BP can be minimized by having a roll rotation during the first period and a pitch rotation during the second period. At the same time, having a pitch rotation during the first and a roll rotation during the second period will be of the greatest disadvantage to a pilot and induce the maximum drop in

P517312.PDF [Page: 74 of 77]

BP during a from hypergravity-hypogravity-hypergravity maneuver. When a pilot is sitting upright and keeping head straight to the front, a rotation of an aircraft will impose the same rotation to the pilot. However, if the pilot turns his/her head to the left or right, this will cause a reorientation of his/her otolithic receptors relative to the acceleration direction. Hence a pitch or roll rotation of the aircraft necessitated by the type of an aerodynamic maneuver a pilots initiates can be potentially synchronized with a pilot's head orientation, effectively resulting in either maximal stimulation of the otolithic receptors (as desired on the transition from hypogravity to hypergravity) or their minimal stimulation (as desired on the transition from hypergravity to hypogravity). Therefore, similar to willingly controlling an anti-G straining maneuver, the pilot may optimally control his/her head direction during aircraft rotation to obtain the desired stimulation of otolith receptors and hence maximize his/her G-tolerance.

Acknowledgment

This work has been supported by the research contract W7711-007683/A issued by the Canadian Department of National Defence, Defence and Civil Institute of Environmental Medicine.

V. REFERENCES

1. AMP Working Group 14. *High G Physiological Protection Training*. Neuilly-sur-Seine, France: NATO-AGARD, 1990; 10; AGARDograph 322.
2. Balaban, CD; Proder, JD. "Neuroanatomic substrates for vestibulo-autonomic interactions." *J Vestibular Res* 1998; 8:7-16.
3. Banks, RD; Grissett, JD; Turnipseed, GT; et al. "The 'push-pull' effect." *Aviat Space Environ Med* 1994; 65:600-704.
4. von Beckh, HJ. "Experiments with animals and human subjects under sub and zero-gravity conditions during the dive and parabolic flight." *J Aviat Med* 1954; 25:235.
5. von Beckh, HJ. "Human reactions during flight to acceleration preceded by or followed by weightlessness." *Aerosp Med* 1959; 30:391-409.
6. Benson, AJ. "Spatial disorientation - general aspects in aviation medicine, physiology and human factors." In: Ernsting, J, ed. **Aviation medicine -- physiology and human factors**. London: William Clowes and Sons Limited; 1978: 405-33.
7. Cheung, BSK; Howard, IP; Money, KE. "Visually induced tilt during parabolic flights." *Exp Brain Res* 1991; 81:391-7.
8. Cheung, BSK; Hofer, K; Goodman, L. "The effects of roll vs. pitch rotation in humans under orthostatic stress." *Aviat Space Environ Med* 1999; 70:966-74.
9. Cowings, PS; Suter, S; Toscano, WB; et al. "General autonomic components of motion sickness." *Psychophysiology* 1986; 23:542-51.
10. Diedrichs, RW. "Adverse effect of negative G_z on subsequent high positive G_z: a need for research and education." *Aeromedical and Training Digest* 1990; 4:36-8.
11. Dobra, N; Reis, DJ. "Role of the cerebellum and vestibular apparatus in regulation of orthostatic reflexes in the cat." *Circ Res* 1974; 34:9-18.
12. Fernandez, C, Goldberg, JM. "Physiology of peripheral neurons innervating semicircular canals of the squirrel monkey II. Response to sinusoidal stimulation and dynamics of the peripheral vestibular system." *J Neurophysiol* 1971; 34:661-75.
13. Fernandez, C; Goldberg, JM. "Physiology of peripheral neurons innervating otolith organs of the squirrel monkey II. Directional selectivity and force response relations." *J Neurophysiol* 1976; 39:970-84.
14. Goldberg, JM; Fernandez, C. "The vestibular system." In: Darian-Smith, I; ed. **Handbook of physiology: Section 1: The nervous system: Volume III, Parts 1 \& 2: Sensory processes**. Oxford: Oxford University Press; 1983: 977-1022.
15. Hu, S; Grant, WF; Stern, RF; Koch, KL. "Motion sickness severity and physiological correlates during repeated exposures to a rotating optokinetic drum." *Aviat Space Environ Med* 1991; 632:308-14.
16. Johnson, W.H.; Sunahara, FA; Landolt, JP. "Motion sickness, vascular changes accompanying pseudo-Coriolis induced nausea." *Aviat Space Environ Med* 1993; 64:367-70.
17. Lehr, AK; Prior, ARJ, Langewouters, G; et al. "Previous exposure to negative G_z reduces relaxed $+G_z$ tolerance." (Abstract #119). *Aviat Space Environ Med* 1992; 63:405.
18. Lestienne, F; Soechting, J; Berthoz, A. "Postural readjustments indued by linear motion of the visual scene." *Exp Brain Res* 1977; 28:363-84.
19. Michaud, VJ; Lyons, TJ; Hansen, CM. "Frequency of the 'push-pull' effect in USAF fighter operations." (Abstract #16). *Aviat Space Environ Med* 1998; 69:201.
20. Ohashi, N; Imamura, J; Nakagawa, H; Mizukoshi, K. "Blood pressure abnormalities as background roles for vertigo, dizziness and disequilibrium." *Otorhinolaryngology* 1990; 52:355.
21. Preber, L. "Vegetative reactions in caloric and rotatory tests." *Acta Otolaryngol Suppl* 1958; 144:1.
22. Prior, ARJ; Adcock, TR; McCarthy, GW. "In-flight arterial blood pressure changes during $-G_z$ to $+G_z$ manoeuvring." (Abstract #55). *Aviat Space Environ Med* 1993; 64:428.
23. Schellong, F. **Regulationsprufung des Kreislaufes**. Darmstadt: Steinkopff, 1954.

P517312.PDF [Page: 75 of 77]

24. Spiegel, EA. "Effects of labyrinthine reflexes on the vegetative nervous system." *Arch Otolaryngol* 1946; 44:61.
25. Steinbacher, BC; Yates, BJ. "Brain stem interneurons necessary for vestibular influences on sympathetic outflow." *Brain Res* 1996; 720:204-10.
26. Sunahara, FA; Farewell, J; Mintz, L; Johnson, WH. "Pharmacological interventions for motion sickness: cardiovascular effects." *Aviat Space Environ Med* 1987; 58(Suppl.): A270-6.
27. Williams, RS; Werchan, PM; Fischer, JR; Bauer, DH. "Adverse effects of G_z in civilian aerobatic pilots." (Abstract #15) *Aviat Space Environ Med* 1998; 69:201.
28. Woodring, SF; Rossiter, CD; Yates, BJ. "Pressor response elicited by nose-up vestibular stimulation in cats." *Exp Brain Res* 1997; 113:165-8.
29. Yates, BJ; Miller, AD. "Properties of sympathetic reflexes elicited by natural vestibular stimulation: implications for cardiovascular control." *J Neurophysiol* 1994; 71:2087-92.
30. Young, LR. "Perception of the body in space: mechanisms." In: Darian-Smith, I; ed. Darian-Smith, I; ed. **Handbook of physiology: Section 1:} The nervous system: Volume III, Parts 1 & 2: Sensory processes**. Oxford University Press: Oxford; 1983: 1023-66.
31. Yates, BJ; Aoki, M; Burchill P; Bronstein, AM; Cresty, MA. "Cardiovascular responses elicited by linear acceleration in humans." *Exp Brain Res* 1999; 125:476-484.
32. Normand, H; Etard, O; Denise P. "Otolithic and tonic neck receptors control of limb blood flow in humans." *J Ame. Physio Soc.* 1997; 1734-38.
33. Wright H. and Buick, F. Measurement of push-pull effect in flight. *Presentation Annual Scientific Meeting, Aerospace Medical Association,* Detroit Michigan, 1999.
34. Yamamoto KI, Kawasaki Y, Izumi R, Kubo T. "Assessment of the otolith-autonomic response using spectral analysis of the R-R interval and blood pressure." *Otolaryngol Hed Neck Surg* 2000 Nov; 123(5):582-6.
35. Grant W, "Otolith Biomechanics." IEEE Engineering in Medicine and Biology Society 10th Annual Int. Conf 1988, 1055
36. Koren, I, Lessard, C.S., "The effect of inertial force acceleration on the otolith membrane." *IEEE Engineering in Medicine and Biology* 2000, 48-55.
37. Matthews, R.S.J., "The G-Excess Effect." *IEEE Engineering in Medicine and Biology* 2000, 56-58.
38. Lee, C.M., Wood, R.H., Welsch, M.A., "Influence of head-down and lateral decubitus neck flexion on heart rate variability." *J Appl Physiol* 2001, 127-32.
39. Ray, C.A., "Interaction of the vestibular system and baroreflexes on sympathetic nerve activity in humans." *Am. J Physiol Heart Circ Physiol* 2000;279:H2399-H2404.
40. Jian, B.J., Cotter, L.A., Emanual, B.A., Cass, S.P., Yates, B.J., "Effects of bilateral vestibular lesions on orthostatic tolerance in awake cats." *J Appl Physiol.* 1999, 86:1552-60.
41. Kerman, I.A., Yates, B.J., "Regional and functional differences in the distribution of vestibulo-sympathetic reflexes." *Am J. Physiol.* 275 (Regulatory Integrative Comp. Physiol. 44) 1998, R824-R835.
42. Kuo, A.D., "An optimal control model of human balance: Can it provide theoretical insight to neural control of movement?" *Proc Amer Control Conf* 1997, 2856-60.
43. Persson, P.B., Kirchheim H.R. (Eds.), Baroreceptor Reflexes: integrative functions and clinical aspects. Springer-Verlag Berlin 1991.
44. Yates, B.J., Holmes M.J., Jian, B.J., "Adaptive placticity in vestibular influences on cardiovascular control." *Brain Res Bull* 2000 Sep. 53(1):3-9.
45. Radtke, A, Popov, K, Bronstein A.M., Gresty M.A., Evidence for a vestibular-cardiac reflex in man." Lancet 2000, 356(9231):736-7.

P517312.PDF [Page: 76 of 77]

DOCUMENT CONTROL DATA SHEET

1a PERFORMING AGENCY

Engineering Services Inc. 1 Bedford Rd, Unit 5 Toronto, Ontario, Canada M5R 2J7

2. SECURITY CLASSIFICATION

UNCLASSIFIED
Unlimited distribution -

1b. PUBLISHING AGENCY

DCIEM

3. TITLE

(U) Dynamic modelling of cardiovascular responses during orthostatic stress

4. AUTHORS

Ziren Lu, William Melek, Alex Kapps

5. DATE OF PUBLICATION

January 7 , 2002

6. NO OF PAGES

63

7. DESCRIPTIVE NOTES

8 SPONSORING/MONITORING/CONTRACTING/TASKING AGENCY

Sponsoring Agency
Monitoring Agency.
Contracting Agency : DCIEM
Tasking Agency

9. ORIGINATORS DOCUMENT NO.

Contract Report CR 2002-08

10. CONTRACT GRANT AND/OR PROJECT NO

W7711-007683/A

11 OTHER DOCUMENT NOS

12. DOCUMENT RELEASABILITY

Unlimited distribution

13 DOCUMENT ANNOUNCEMENT

Unlimited announcement

P517312.PDF [Page: 77 of 77]

14. ABSTRACT

(U) This final report summarized the investigation of a subject's dynamic cardiovascular responses during orthostatic stress. For the purposes of this investigation, a toolbox dubbed CROST (Countermeasures Research on Orthostatic Stress) has been designed. The toolbox automatically generates and statistically analyzes dynamic models that reveal the dynamic behavior of the cardiovascular system during pitch and roll rotations: models for up/down tilt, pitch/roll rotations, different tilt onset/offset rates, and dwell times. The blood pressure dynamics is characterized by the physiologically significant indices associated with the models. Furthermore, using maneuver profile data, such as tilt orientation (pitch or roll), tilt direction (up or down), rotation rate (15, 30, 45 deg/sec) and head-down dwell time (7, 15, 30 sec) as well as the physiological indices, a set of fuzzy logic models is generated automatically by CROST. These dynamic and fuzzy-logic models assist in providing an operationally important predictive view on the characteristics of blood pressure responses to orthostatic stress induced by pitch and roll rotations. Repeated measures analysis of variance has shown that the magnitude of blood pressure decrease induced by head-down tilt is significantly higher ($p < 0.05$) in pitch than in roll rotation, whereas the blood pressure decrease induced by the head-up (HU) rotation is significantly higher ($p < 0.05$) in roll than in pitch. The tilt orientation and rotation rate also have a significant effect on blood pressure dynamics. Our results demonstrate that the roll rotation to hypogravity followed by the pitch rotation back to hypergravity will induce the least decrease in a subject's blood pressure, thereby maximizing the subject's G-tolerance. The working hypothesis analyzed in this project is that the results can be explained on the basis of well-known otolith-cardiovascular reflex and bi-directional sensitivity of vestibular otolith organs that contribute to blood pressure compensation during pitch, but not during roll rotations.

15 KEYWORDS, DESCRIPTORS or IDENTIFIERS

(U) G transition, modelling, cardiovascular

#517312
CA020599